

Accepted Manuscript

Discovery of *in vitro* antitubercular agents through *in silico* ligand-based approaches

Daniela De Vita, Fabiana Pandolfi, Roberto Cirilli, Luigi Scipione, Roberto Di Santo, Laura Friggeri, Mattia Mori, Diego Fiorucci, Giorgio Maccari, Robert Selwyne Arul Christopher, Claudio Zamperini, Valentina Pau, Alessandro De Logu, Silvano Tortorella, Maurizio Botta



PII: S0223-5234(16)30428-7

DOI: [10.1016/j.ejmech.2016.05.032](https://doi.org/10.1016/j.ejmech.2016.05.032)

Reference: EJMECH 8624

To appear in: *European Journal of Medicinal Chemistry*

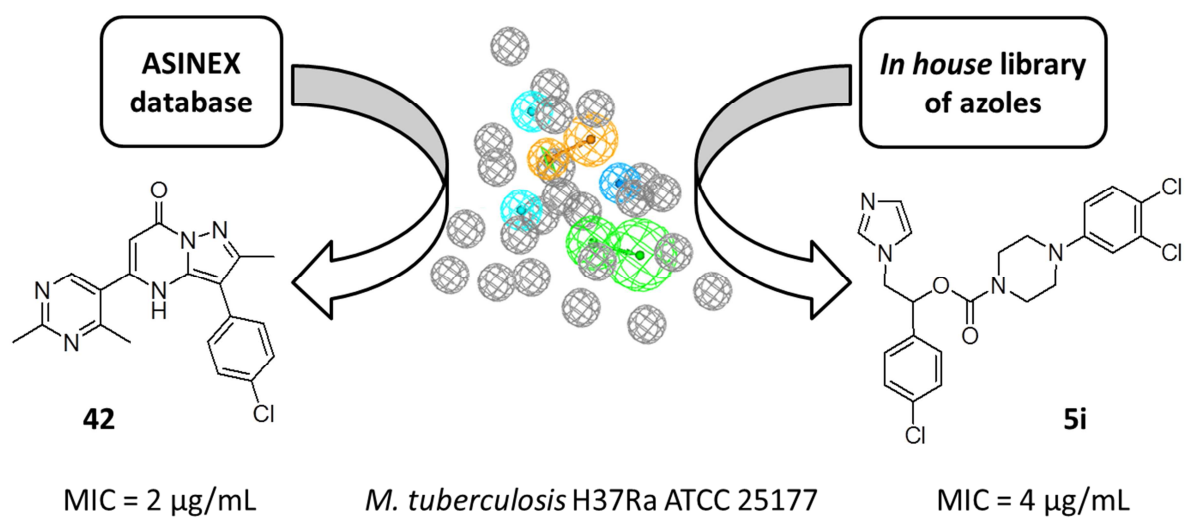
Received Date: 23 March 2016

Revised Date: 12 May 2016

Accepted Date: 16 May 2016

Please cite this article as: D. De Vita, F. Pandolfi, R. Cirilli, L. Scipione, R. Di Santo, L. Friggeri, M. Mori, D. Fiorucci, G. Maccari, R.S.A. Christopher, C. Zamperini, V. Pau, A. De Logu, S. Tortorella, M. Botta, Discovery of *in vitro* antitubercular agents through *in silico* ligand-based approaches, *European Journal of Medicinal Chemistry* (2016), doi: 10.1016/j.ejmech.2016.05.032.

This is a PDF file of an unedited manuscript that has been accepted for publication. As a service to our customers we are providing this early version of the manuscript. The manuscript will undergo copyediting, typesetting, and review of the resulting proof before it is published in its final form. Please note that during the production process errors may be discovered which could affect the content, and all legal disclaimers that apply to the journal pertain.



ACCEPTED MANUSCRIPT

Discovery of *in Vitro* Antitubercular Agents Through *in Silico* Ligand-Based Approaches

Daniela De Vita,^[a] Fabiana Pandolfi,^[a] Roberto Cirilli,^[b] Luigi Scipione,^[a] Roberto Di Santo,^[a,c] Laura Friggeri,^[a] Mattia Mori,^[d,e] Diego Fiorucci,^[d] Giorgio Maccari,^[d] Robert Selwyne Arul Christopher,^[d] Claudio Zamperini,^[d] Valentina Pau,^[g] Alessandro De Logu,^[g] Silvano Tortorella,*^[a] and Maurizio Botta*^[d,f]

^[a] Dipartimento di Chimica e Tecnologie del Farmaco, Sapienza Università di Roma, Piazzale Aldo Moro 5, 00185 Roma (Italy)

^[b] Dipartimento del Farmaco, Istituto Superiore di Sanità, Viale Regina Elena 299, 00161 Roma (Italy)

^[c] Istituto Pasteur-Fondazione Cenci Bolognetti, Dipartimento di Chimica e Tecnologie del Farmaco, Sapienza Università di Roma, Piazzale Aldo Moro 5, 00185 Roma (Italy)

^[d] Dipartimento di Biotecnologie, Chimica e Farmacia, Università degli Studi di Siena, Via Aldo Moro 2, 53019 Siena (Italy)

^[e] Center for Life Nano Science@Sapienza, Istituto Italiano di Tecnologia, viale Regina Elena 291, 00161 Roma (Italy)

^[f] Sbarro Institute for Cancer Research & Molecular Medicine, Center for Biotechnology, College of Science & Technology, Temple University, BioLife Science Building, Suite 333, 1900 N 12th Street, Philadelphia, PA 19122 (USA)

^[g] Dipartimento di Scienze della Vita e dell'Ambiente, Università degli Studi di Cagliari, Via Porcell 4, 09124 Cagliari, Italy

* Corresponding authors: maurizio.botta@unisi.it; silvano.tortorella@uniroma1.it

Abstract

The development of new anti-tubercular agents represents a constant challenge mostly due to the insurgency of resistance to the currently available drugs. In this study, a set of 60 molecules were selected by screening the Asinex and the ZINC collections and an *in house* library by means of *in silico* ligand-based approaches. Biological assays in *M. tuberculosis* H37Ra ATCC 25177 strain highlighted (\pm)-1-(4-chlorophenyl)-2-(1*H*-imidazol-1-yl)ethyl-4-(3,4-dichlorophenyl)piperazine-1-carboxylate (**5i**) and 3-(4-chlorophenyl)-5-(2,4-dimethylpyrimidin-5-yl)-2-methylpyrazolo[1.5-a]pyrimidin-7(4*H*)-one (**42**) as the most potent compounds, having a Minimum Inhibitory Concentration (MIC) of 4 and 2 $\mu\text{g/mL}$ respectively. These molecules represent a good starting point for further optimization of effective anti-TB agents.

Keywords

Virtual screening; anti-tubercular agents; azoles; phenyl-pyrazolopyrimidinones.

Highlights

- A refined anti-tubercular pharmacophore model was described;
- 60 molecules were selected by virtual screening of commercial and in house library;
- Anti-tubercular activity was evaluated on hit compounds;
- Two new lead compounds were identified with 2 and 4 $\mu\text{g/mL}$ MIC.

1. Introduction

Tuberculosis (TB) is a widespread infectious disease caused by the bacillus *Mycobacterium tuberculosis*. It typically affects the lungs (pulmonary TB) but can also affect other parts of the body (extrapulmonary TB). *M. tuberculosis* is spread from person to person through the air when people with pulmonary TB expel bacteria, by coughing and sneezing.[1] To date, TB remains a major global health problem and it is responsible for a large number of deaths. According to the latest projections worldwide, 9.6 million people are estimated to have fallen ill with TB in 2014: 5.4 million men, 3.2 million women and 1.0 million children. Globally, 12% of the 9.6 million new TB cases in 2014 were HIV-positive.[1] Generally, a relatively small proportion of people infected with *M. tuberculosis* will develop the disease. It is estimated that one-third of the global population is infected without evidence of clinically manifested active TB (latent TB infection).[2] In this form, *M. tuberculosis* lives in a non-replicating stage in lungs' cavities with caseous necrosis and poor access to oxygen[3] and infected people do not have TB disease and symptoms.[4] Therefore, people with latent form are often treated to prevent the development of active TB.[5] The current treatment of active and latent TB consists in a drugs combination (isoniazid, rifampicin, rifapentine, ethambutol and pyrazinamide) administered over six months. Long treatment period and poor patients' adherence to the current treatment lead to the emergence of *M. tuberculosis* strains resistant to some or all available anti-TB drugs, called MDR (multidrug-resistant), XDR (extensively drug resistant) and TDR (totally drug resistant) could arise.[5, 6]

In 2012, the diarylquinoline bedaquiline has been approved by US Food and Drug Administration as part of combination therapy to treat MDR pulmonary TB.[7] Nevertheless, based on the overall limitations described above, new antibiotics to treat TB infection are urgently needed.

Recently, many successful examples of anti-TB hit and lead compounds have been reported by many research groups,[8-11] including our own. In particular, the identification of new anti-TB compounds with innovative structures has been pursued by ligand-based molecular modeling tools such as pharmacophore models, which have been used for screening virtual libraries of small molecules and to drive the rational optimization of hit and lead candidates. In brief detail, a 5-hydroxy-pyrazole compound,[12] characterized by a MIC of 25 $\mu\text{g}/\text{mL}$, first emerged as a hit candidate from virtual screening. Subsequent optimization of the hit and synthesis of a library of derivatives led us to obtain pyrazoles,[13] pyrazolone,[14] andazole analogues with polycyclic structures[15] as interesting compounds with enhanced anti-TB activity and endowed with MIC values ranging between 4 and 12 $\mu\text{g}/\text{mL}$. In addition, a series of pyrrole derivatives endowed with strong anti-TB activity and MIC values lower than 0.125 $\mu\text{g}/\text{mL}$ have been also developed by pharmacophore modeling.[16, 17] However, as implicit in most common ligand-based approaches, the macromolecular target(s) for these classes of hit and lead compounds is still unknown and, for the moment, only a few hypotheses on the possible mechanism of action have been formulated.[16, 17] Nevertheless, these pharmacophores proved to be highly efficient in identifying hit compounds endowed with anti-TB activity and having different chemical composition, as well as in driving the optimization of these hits up to valuable lead compounds.[16, 17]

By following our research interest in developing anti-TB lead compounds and our research strategies relying on pharmacophore modeling and screening, here we describe a new pharmacophore model that was obtained by refining the previous ligand-based pharmacophores based on literature data. Accordingly, this work represents the logical prosecution of the previous ligand-based studies performed by our own research group.[12-17] First, two chemical libraries were screened through the above pharmacophore, namely i) the Asinex database of commercially available compounds, and

ii) our *in house* library including azole derivatives previously synthesized as antifungal and antiprotozoal agents. The first set of molecules was further optimized *in silico* by screening the ZINC database in a ligand-based strategy. The second set of molecules has been included because recently some azole antifungal agents have been described to possess also anti-TB activity, thus highlighting the potentiality for exploiting the azole scaffold in anti-TB medicinal chemistry.[18] Virtual hits have been tested *in vitro* in a model of TB infection and rough structure-activity relationships (SAR) have been afforded for two different series of molecules, most probably endowed with two different mechanisms of action but providing remarkable anti-TB effects *in vitro*.

2. Results and Discussion

2.1. Generation of a common feature pharmacophore model

A total of 71 small molecules, which have been synthesized in our group and already described in previous publications as inhibitors *in vitro* of the growth of *M.tuberculosis* H37Rv ATCC 27294 strain were collected and used as training set.[12-17] Notably, these molecules were tested *in vitro* by the same research group in the same experimental condition, thus allowing the generation of a reliable and unbiased ligand-based pharmacophore model. Out of these 71 small molecules, those having a MIC < 12 µg/mL were arbitrarily classified as “active”, those having a MIC comprised between 12 and 32 µg/mL were arbitrarily classified as moderately active, whereas those having a MIC > 32 µg/mL were considered as inactive during the generation of the common feature pharmacophore model. No further descriptors were considered in this classification, thus allowing the generation of a pharmacophore model composed of conventional features as well as exclusion volumes, which are placed according to the biological activity of compounds in the training set (Figure 1).

Our pharmacophoric analysis was carried out using the *CATALYST-HipHop* procedure, which evaluates the common features and the hypothetical ideal geometry of compounds included in the training set ligands. This was performed in a three step procedure that led to the generation of a number of common feature pharmacophore models. The highest ranked pharmacophore hypothesis, which was composed of 5 features (1 Ring Aromatic (RA), 1 H-Bond Acceptor (HBA), 2 Hydrophobic Aromatic (HydArom1 and HydArom2) and 1 Hydrophobic aliphatic (HydAli)) and 23 excluded volumes (Figure 1), proved to map perfectly the most potent compounds of the training set (Figure 1), and was therefore selected as query in virtual screening.

[figure 1]

2.2. Virtual screening

The whole ASINEX database collection (757900 compounds) and an *in house* library ofazole compounds were screened towards the selected pharmacophore model, with the aim to identify new chemotypes of *M. tuberculosis* inhibitors. Pharmacophore screening was performed with Discovery Studio from Accelrys[19] and filtered ligands were sorted according to the FitValue score.

By screening the ASINEX database, 28298 compounds having FitValue above 2.50 were filtered by the pharmacophore (3.7% of the ASINEX database). Since the cell wall of *M. tuberculosis* is known to be noticeably hydrophobic, highly aqueous soluble molecules were discarded by setting logP filter greater than 4.50, thus retaining 10486 compounds (1.43% of the ASINEX database). Further, the number of compounds was reduced through shape similarity searching performed by Discovery Studio. In particular, the shape of the most potent compound included in the training set (MIC = 0.125 µg/mL, Supporting Information) was used to filter the remaining 10486 small molecules. Out of them, 575 compounds having at least 50% shape similarity (Tanimoto score higher than 0.5) with the

most active compound were selected. The final shortlist of compounds was achieved by visual inspection of the pharmacophoric alignment of these molecules as well as by considering structural diversity and custom filters. In detail, based on previous works performed by our own group that highlighted the *para*-chlorophenyl system as crucial for activity,[13] scaffolds having the *para*-chlorophenyl moiety mapping to the RA feature (Figure 1) were deemed top priority. In addition, scaffolds having a Sulphur atom mapping to the HBA feature were discarded, because of the weak tendency to accept H-bond of Sulphur,[20, 21] while compounds having a chiral center with unspecified geometry (most likely they are sold as a racemic mixture) were selected only if both enantiomers were able to map satisfactorily the pharmacophore model. This selection led to a final list of 27 small molecules, namely **10-36** that were purchased from Asinex and tested *in vitro* (see Supporting Information).

The *in house* library of 96 azole compounds was screened by using the same procedure described above and detailed in the Experimental Section. In this particular case, based on the limited dimension of the screening library, the filter based on the molecular shape of the most potent anti-TB compound included within the training set was not applied. Indeed, the compounds endowed with the highest FitValue after pharmacophore screening, namely **1-4**, **5a-f,l** and **7** were selected and submitted to *in vitro* tests. Considering the reduced structural differences in the phenyl moiety of the 2-(1*H*-imidazol-1-yl)-1-phenylethanol derivatives analyzed by the pharmacophoric model, we decided to enlarge the set of studied compounds exploring more substituents, such as a bulky lipophilic ring *i.e.* naphthyl and biphenyl (**5n** and **6**) or a small and polar nitro group (**5m**).

2.3. Biological activity

Minimum Inhibitory Concentration (MIC) of each tested compound against *M. tuberculosis* H37Ra ATCC 25177 was determined by the agar dilution method, as previously reported

with slight modifications.[22] The biological assays results are reported in Table 1. Overall, the most promising molecule selected by virtual screening of the ASINEX database of commercially available compounds was **24**, which inhibited the growth of *M. tuberculosis* with a MIC of 8 µg/mL, and was therefore selected as hit compound for further deepening of the phenyl-pyrazolopyrimidinone scaffold (see below). In contrast screening the *in house* library of azole compounds provided **5i** as the most potent compound, having a MIC of 4 µg/mL. This molecule was further investigated, in order to depict the possible mechanism of action of this series (see below).

2.4. Synthesis of azole derivatives

The azole derivatives were prepared as racemates or as (*S*)-enantiomers, according to suggestions coming from pharmacophore screening. Generally the azoles were prepared following the same procedure, however for synthesizing 2-(1*H*-imidazol-1-yl)-1-phenylethanols as racemic mixture the ketone group was reduced to alcohol using NaBH₄, while RuCl(p-cymene)[(*R,R*)-Ts-DPEN] was used for preparing (*S*)-2-(1*H*-imidazol-1-yl)phenylethanols differently substituted.[23, 24] The final azoles (with the exception of (*S*)-**5n**) were synthesized using two different procedures, Method A or B. (Scheme 1). In particular the activation of the alcohol group was performed using NaH, (Method A) or triphosgene (Method B).[25, 26] More details are described in experimental section.

[Scheme 1]

Compounds (**S**)-**5n**, was prepared by activation of the amino function of 1-(3,4-dichlorophenyl)piperazine using triphosgene and pyridine; then, the corresponding 4-(3,4-dichlorophenyl)piperazine-1-carbonyl chloride was condensed with 1-([1,1'-biphenyl]-4-yl)-2-(1*H*-imidazol-1-yl)ethanol (**51**) (Scheme 2). Finally, **8** and **9** were synthesized by condensation of alcohols **53** and **54** respectively with 4-(3,4-dichlorophenyl)piperazine-1-carbonyl chloride (Scheme 2). The 1-(4-chlorophenyl)-2-phenylethanol **53** was obtained by

reduction with NaBH₄ of commercial 1-(4-chlorophenyl)-2-phenylethanone. Otherwise, the 1-(4-chlorophenyl)-2-(1H-pyrrol-1-yl)ethanol **54** was prepared starting from hexamethylenetetramine and 2-bromo-1-(4-chlorophenyl)ethanone and subsequent treatment with HCl 37% in EtOH. The corresponding oxoethanaminium was reacted with 2,5-dimethoxytetrahydrofuran according to the Clauson-Kaas procedure,[27] then 1-(4-chlorophenyl)-2-(1H-pyrrol-1-yl)ethanone was reduced to **54** with NaBH₄.

[Scheme 2]

2.5. SAR analysis for the azole derivatives

All tested azole derivatives share the common 2-(1H-imidazol-1-yl)-1-phenylethanol moiety; the main structural differences regarding: i) the length and polarity of the side chain, comprising esters (**1,4-7**) and carbamates (**5a-m,6**); ii) substitution of the aromatic ring of the 1-phenylethanol moiety.

The activity data show that the compounds with the same 2-(1H-imidazol-1-yl)-1-phenylethanol moiety and different side chain have activities ranging from 4 to 64 µg/mL suggesting that the modification of the side chain is an extremely important factor for obtaining variations of the *in vitro* biological activity.

Furthermore, it was generally observed that the presence of a *para*-chloro substituent produces an improvement of activity compared to a *para*-fluoro group (**5c** vs **5d**, **5i** vs **5h**) in compound series with an identical side chain, and this was in agreement with our previous findings.[13] Whereas, the presence of a second chlorine atom in the *ortho*-position such as in (S)-**5l** reduces the anti-TB activity with respect to **5i**. Moreover, the replacement of the *para*-chloro of **5i** with a *para*-nitro group [(S)-**5m**], a phenyl group [(S)-**5n**] or the substitution of the phenyl ring with naphthyl [(S)-**6**] invariably reduced the anti-TB potency.

Modifications of the 2-(1*H*-imidazol-1-yl)-1-phenylethanol moiety led to a major changes in the biological activity. Indeed, the replacement of imidazole ring of **5i** with phenyl (compound **8**) or a pyrrole (compound **9**) resulted in a loss of activity against *M. tuberculosis*.

2.6. Metabolic stability assay of **5i**

In vitro metabolic stability was experimentally evaluated for the most interesting compound (**5i**) in order to have a reliable indication of its plasma level after oral administration.

The metabolic stability reported in Table 2 is expressed as percentage of the unmodified parent drug remaining in the mixture while the metabolites (M1) were separated in HPLC and analysed via mass spectrometry. The information on the metabolite mass obtained with the latter spectroscopic studies were then integrated with the *in silico* metabolites prediction obtained with the software Metasite[28-30] thus allowing us to confirm the structure of each metabolite (metabolites structures are reported in the Figure S5, Supporting Information).

[Table 2]

This compound shows a high metabolic stability in this experimental condition. Only one metabolite was observed, that is the product of the CYP-dependent mono-oxygenation reaction at the α carbon position. This metabolite was found to be the 1% of the unmodified parent drug. Moreover, experimental metabolite M1 was correctly predicted by Metasite and ranked in the top six positions.

2.7. Optimization of the 3-phenylpyrazolo[1-5a]pyrimidin-7(4H)-one scaffold and SAR analysis

The 3-phenylpyrazolo[1-5a]pyrimidin-7(4H)-one derivative **24** showed a good anti-TB activity when compared to other compounds resulting from the pharmacophoric approach. Accordingly, with the aim to improve its anti-TB activity, a number of chemical modifications of this scaffold were planned. To this end, we used the shape matching method implemented in the ROCS program.[31, 32] Starting from our hit compound **24**, we performed a survey of the available literature and found that three additional molecules belonging to the same scaffold and endowed with anti-TB activity have been disclosed by Mao et al. and Ananthan et al. (Figure 2A).[33, 34] These molecules and **24** were thus used to create a shape query by means of the vROCS program (Figure 2A, B). The four molecules were aligned using an in house developed python script which superimposes the heavy atoms keeping the best combination in term of physicochemical features. This alignment output was used for the query generation. The selection of the biological active conformation is not possible for these molecules because the target is unknown. However, since they have less than four rotatable bonds, the possible conformations are limited and very similar between themselves. Thus, a conformation that could be adopted by all the active molecules was trusted as reliable.

[Figure 2]

The query was validated as described in the Supporting Information, and used to virtually screening the “All now” subset of the ZINC database (approx. 9 million compounds).[35] This database was pre-filtered using Filter program,[36, 37] part of the OpenEye Suite, with a modified version of the drug-like ruleset to retain molecules with a higher probability of becoming an antitubercular agent. In particular, we reduced the minimum molecular weight of the compounds that could pass the filter, increased ClogP value and filtered out molecules with reactive or unwanted features. The rationale behind the increase of the ClogP value was the need to select molecules able to cross the thick and lipophilic barrier

of the *M. tuberculosis*. After filtration, the remaining 5250000 molecules were submitted to conformational analysis by Omega2 (OpenEye suite), [36, 37] and were screened towards the ROCS query. The first 5000 molecules sorted by the TanimotoCombo score were selected and visually inspected. Among them, the 13 most promising compounds, namely **37–49** (Figure 2C and Supporting Information), were selected by taking into account the decoration of the scaffold, with particular attention to the variable part of the four molecules used to build our query (Figure 2A). Indeed, **37–49** bear aromatic substituents directly linked to the scaffold, or aromatic substituents linked through linker of varying length, or substituents with aliphatic chains or aliphatic rings. Bioassays showed that some of these molecules have activity in the 8-16 $\mu\text{g/mL}$ range, comparable with the starting hit **24** (Table 3). Interestingly, molecule **42** showed activity of 2 $\mu\text{g/ml}$ representing a substantial improvement of the starting hit **24** (Table 3 and Figure 2C).

After hit optimization, we produced a simple structure activity relationship the 3-phenylpyrazolo[1-5a]pyrimidin-7(4H)-one scaffold (Figure 3). The aliphatic substituents in -R (Figure 3) not improved the activity, while the use of an etheric function provided anti-TB activity comparable to the hit compound **24**. In the same position -R, some aliphatic linkers connecting an aromatic substituents were introduced, providing anti-TB activity comparable to the starting hit compound, whereas the introduction of a dimethyl pyrimidine moiety led to the best anti-TB activity of the series. The replacement of the methyl group in -R¹ with hydrogen, substituted phenyl rings and a methoxymethyl chain, proved to be ineffective. In the R² position the electron withdrawing chlorine atom was substituted with one or two electron donor O-methyl groups or with hydrogen. All these modifications did not improve the anti-TB activity of **24**. Overall, the most relevant modification was the insertion of a dimethyl pyrimidine substituent on the R position, which led to the compound **42** that is endowed with a MIC of 2 $\mu\text{g/mL}$.

[Figure 3]

3. CONCLUSIONS

In this work, the Asinex database of commercially available compounds and an *in house* library of azoles were screened *in silico* through a pharmacophore model. A set of 47 molecules were first selected and investigated *in vitro* as candidate inhibitors of the growth of *M. tuberculosis* H37Ra ATCC 25177.

The screening of the azole library provided **5i** as the most promising compound, having a MIC of 4 µg/mL. All the screened azoles possess a 2-(1*H*-imidazol-1-yl)-1-phenylethanol skeleton and the main structural diversity concerns the side chain linked to the alcohol or the 1-phenylethyl moiety. Side chain modification can produce pronounced differences in anti-TB activity; compounds with the same 2-(1*H*-imidazol-1-yl)-1-phenylethanol moiety and different side chain have activities ranging from 4 to 64 µg/mL

Moreover, it was generally observed that, in compounds with the same side chain, the presence of a *para*-chloro substituent produces an improvement of activity compared to *para*-fluoro group (**5c** vs **5d**, **5i** vs **5h**). Furthermore, the introduction of a second chlorine atom in the *ortho*-position such as (S)-**5l** reduces the anti-TB activity with respect to **5i**. The substitution of the *para*-chloro group of **5i** with *para*-nitro or phenyl group such as in (S)-**5m** and (S)-**5n** reduced the anti-TB potency as well as the substitution of the phenyl ring of **5i** with naphthyl moiety [(S)-**6**]. The replacement of imidazole ring of **5i** with phenyl (compound **8**) or a pyrrole (compound **9**) resulted in a loss of activity against *M. tuberculosis*.

Compound **24** was found as the most active compound among the ASINEX database with a MIC of 8 µg/mL and was therefore selected as hit for further deepening of the 3-phenylpyrazolo[1-5a]pyrimidin-7(4H)-one scaffold. Starting from **24** and three analogues

endowed with anti-TB activity retrieved from the literature, a shape- and chemistry-based query was built with ROCS. Screening the ZINC database with this query provided 13 compounds (**37-49**), which were selected taking into account the variations in the decoration of the scaffold. Some of these molecules showed an *in vitro* antitubercular activity in the 8-16 $\mu\text{g/mL}$ range, comparable with the starting hit **24**. Interestingly, **42** represented a significant improvement of the starting hit **24** with an activity of 2 $\mu\text{g/mL}$.

In conclusion, we have identified two new hits showing a good anti-mycobacterial activity *in vitro*, which are attractive candidates for further development of new anti-tubercular agents.

4. Experimental Section

4.1. Chemistry

General: All reagents and solvents were of high analytical grade and were purchased from Sigma-Aldrich (Milano, Italy). The 2-(1*H*-imidazol-1-yl)-1-arylethanones and racemic 2-(1*H*-imidazol-1-yl)-1-phenylethanols were prepared according to literature procedure.[23] Melting points were determined on Tottoli (Buchi) or Kofler apparatus (where specified) and are uncorrected. Infrared spectra were recorded on a Spectrum One ATR Perkin Elmer FT-IR spectrometer. NMR spectra were acquired on a Bruker AVANCE-400 or AVANCE-200 spectrometer in DMSO- d_6 , CD₃OD or CDCl₃ at 27 °C; chemical shift values are given in δ (ppm) relatively to TMS as internal reference. Coupling constants are given in Hz. Abbreviations: s=singlet, d=doublet, t=triplet, q=quartet, m=multiplet, dd=doublet of doublet. Mass spectrometric experiments were carried out with a 2000 Q TRAP instrument (Applied Biosystems); a commercial hybrid triple-quadrupole linear ion-trap mass spectrometer (Q1q2QLIT), equipped with an ESI source and a syringe pump have been used. The examined compounds were previously dissolved in methanol (10^{-5} M) and

aqueous HCl was added just before the injection. The molecular peaks (m/z) have been observed as $[M+H]^+$; for chlorine containing compounds, the highest intensity peak was reported. Elemental analyses were obtained by a PE 2400 (Perkin-Elmer) analyzer and the analytical results were within $\pm 0.4\%$ of the theoretical values for all compounds. The analytical HPLC apparatus consisted of a PerkinElmer (Norwalk, CT, USA) 200 LC pump equipped with a Rheodyne (Cotati, CA, USA) injector, a 20 μ L sample loop, an HPLC Dionex CC-100 oven (Sunnyvale, CA, USA) and a Jasco (Jasco, Tokyo, Japan) Model CD 2095 Plus UV/CD detector. Chiral HPLC analysis were performed using the commercially available column Chiralpak IC (250 mm x 4.6 mm i.d.) and Chiralpak IB-3 (250 mm x 4.6 mm i.d.).

4.1.1. (\pm)-1-(4-chlorophenyl)-2-(1*H*-imidazol-1-yl)ethyl-2-phenoxyacetate (1):

Sodium hydride (13 mg, 0.54 mmol) was added to a suspension of (\pm)-1-(4-chlorophenyl)-2-(1*H*-imidazol-1-yl)ethanol (120 mg, 0.54 mmol) in dry CH_3CN (5 mL). After 2 h at RT, the phenoxyacetyl chloride (220 μ L, 1.59 mmol) was dropwise added and the reaction mixture was stirred overnight at RT. The solvent was removed under reduced pressure and the obtained residue was dissolved in CH_2Cl_2 (10 mL) and washed with saturated Na_2CO_3 solution (2 x 10 mL). The separated organic layer was dried over Na_2SO_4 and evaporated under reduced pressure. The residue was crystallized from EtOAc to give pure **1** as a white solid (183 mg, 95%); mp: 103-105 $^\circ\text{C}$; IR (neat, ν cm^{-1}): 1751(C=O); ^1H NMR (400 MHz, $\text{DMSO}-d_6$) δ (ppm): 4.42 (d, $J = 5.5$ Hz, 2H), 4.83 (d, $J = 16.7$ Hz, 1H), 4.91 (d, $J = 16.7$ Hz, 1H), 6.11 (t, $J = 5.5$ Hz, 1H), 6.82-6.87 (m, 3H), 6.97 (t, $J = 7.4$ Hz, 1H), 7.13 (s, 1H), 7.27 (dd, $J = 8.5, 7.4$ Hz, 2H), 7.35 (d, $J = 8.5$ Hz, 2H), 7.43 (d, $J = 8.5$ Hz, 2H), 7.54 (s, 1H); MS (ESI): m/z calcd for $\text{C}_{19}\text{H}_{17}\text{ClN}_2\text{O}_3$: 357.10 $[M+H]^+$, found 356.90; Anal. calcd for $\text{C}_{19}\text{H}_{17}\text{ClN}_2\text{O}_3$: C 63.96, H 4.80, N 7.85, found: C 63.86, H 4.81, N 7.83.

4.1.2. (S)-1-(4-fluorophenyl)-2-(1H-imidazol-1-yl)ethyl-(3-(1H-imidazol-1-yl)propyl)carbamate [(S)-2]:

(S)-1-(4-fluorophenyl)-2-(1H-imidazol-1-yl)ethanol (100 mg, 0.48 mmol) was suspended in 5 mL of dry CH₃CN, then triphosgene (71 mg, 0.24 mmol) was added. The mixture was stirred overnight at RT. The reaction mixture was treated with Et₂O, until the complete precipitation of a white solid. The solvent was removed by decantation; the white solid was washed with Et₂O (2 × 5 mL) and dissolved in anhydrous CH₃CN. Then, TEA (222 μL, 1.6 mmol) and 3-(1H-imidazol-1-yl)propan-1-amine (95 μL, 0.8 mmol) were added. The reaction was stirred overnight at RT. The crude mixture was diluted with H₂O (5 mL), and the aqueous layer was extracted with CHCl₃ (3 × 10 mL). The combined organic layers, dried under Na₂SO₄, were evaporated under reduced pressure. The crude product was purified by silica gel column chromatography (CH₂Cl₂ / MeOH 80:20) to give (S)-2 (138 mg, 80%, e.e.>99%); mp: 101-103 °C; IR (neat, ν cm⁻¹): 1710 (C=O); ¹H NMR (400 MHz, CD₃OD) δ (ppm): 1.93 (m, *J* = 6.8 Hz, 2H), 3.05 (m, 2H), 4.00 (t, *J* = 6.8 Hz, 2H), 4.40 (m, 2H), 5.92 (m, 1H), 6.94 (s, 1H), 6.96 (s, 1H), 7.11 (m, 4H), 7.36 (m, 2H), 7.56 (s, 1H), 7.62 (s, 1H); ¹³C NMR (100 MHz, CDCl₃) δ (ppm): 31.2, 38.1, 44.4, 52.0, 74.1, 115.8 (*J* = 22.0 Hz), 118.8, 119.8, 128.0 (*J* = 8.0 Hz), 128.9, 129.3, 133.0 (*J* = 2.0 Hz), 137.2, 137.9, 155.2, 162.8 (*J* = 247.0 Hz); MS (ESI): *m/z* calcd for C₁₈H₂₀FN₅O₂: 358.17 [M+H]⁺, found: 358.13; Anal. calcd for C₁₈H₂₀FN₅O₂: C 60.49, H 5.64, N 19.60, found: C 60.49, H 5.65, N 19.63.

4.1.3. (S)-1-(4-chlorophenyl)-2-(1H-imidazol-1-yl)ethyl-3-(trifluoromethyl) benzoate [(S)-3]:

Sodium hydride (13 mg, 0.54 mmol) was added to a stirred suspension of (S)-1-(4-chlorophenyl)-2-(1H-imidazol-1-yl)ethanol (120 mg, 0.54 mmol) in dry CH₃CN(5 mL). After 2 h at RT the sodium alkoxide was treated with 3-(trifluoromethyl)benzoyl chloride (111 μL,

0.75 mmol). The reaction mixture was stirred for 24 h at RT. The solvent was removed under reduced pressure and the residue was treated with CH₂Cl₂ (20 mL) and washed with saturated Na₂CO₃ solution (2x10mL). The organic layer, dried over Na₂SO₄, was evaporated under reduced pressure. The crude yellow oil was purified by silica gel column chromatography using CH₂Cl₂ / MeOH 90:10 as eluent to obtain (S)-**3** as colorless oil (114 mg, 56%, e.e.>99%); IR (neat, ν cm⁻¹): 1729 (C=O); ¹H NMR (400 MHz, CDCl₃) δ (ppm): 4.48-4.41 (m, 2H), 6.20 (t, J = 5.3 Hz, 1H), 6.86 (s, 1H), 7.04 (s, 1H), 7.21-7.28 (m, 2H), 7.35-7.39 (m, 3H), 7.64 (t, J = 7.8 Hz, 1H), 7.88 (d, 1H, J = 7.8 Hz), 8.22 (d, J = 7.8 Hz, 1H), 8.29 (s, 1H); MS (ESI): m/z calcd for C₁₉H₁₄ClF₃N₂O₂: 395.08 [M+H]⁺, found: 395.00; Anal. calcd for C₁₉H₁₄ClF₃N₂O₂: C 57.81, H 3.57, N 7.10, found: C 57.89, H 3.56, N 7.12.

4.1.4. (S)-1-(4-fluorophenyl)-2-(1*H*-imidazol-1-yl)ethyl (4-isopropylphenyl)carbamate [(S)-**4**]:

Sodium hydride (13 mg, 0.53 mmol) was added to a suspension of (S)-1-(4-fluorophenyl)-2-(1*H*-imidazol-1-yl)ethanol (110 mg, 0.53 mmol) in dry CH₃CN (5 mL). After 2 h at RT, 4-isopropylphenyl isocyanate (254 μ L, 1.59 mmol) was added and the suspension was stirred for 24 h at RT. The solvent was evaporated under reduced pressure, and the solid residue was washed with MeOH (3x3 mL). The mother liquor was dried and purified by silica gel column chromatography (CH₂Cl₂ / MeOH 90:10) to give (S)-**4** as a white solid (88 mg, 45%, e.e. > 99%); mp: 200-202 °C; IR (neat, ν cm⁻¹): 1715 (C=O); ¹H NMR (400 MHz, CD₃OD) δ (ppm): 1.22 (d, J = 6.9 Hz, 6H), 2.85 (m, 1H), 4.44 (m, 2H), 6.00 (t, J = 5.4 Hz, 1H), 6.94 (s, 1H), 7.08-7.15 (m, 5H), 7.30 (d, J = 8.5 Hz, 2H), 7.38 (m, 2H), 7.57 (s, 1H); ¹³C NMR (100 MHz, CD₃OD) δ (ppm): 23.1, 33.4, 51.2, 74.2, 115.1 (J = 21.0 Hz), 118.7, 120.2, 126.3, 127.4, 128.0 (J = 9.0 Hz), 133.6 (J = 3.0 Hz), 136.0, 137.8, 143.8, 153.0, 162.7 (J = 245.0 Hz); MS (ESI): m/z calcd for C₂₁H₂₂FN₃O₂: 368.18 [M+H]⁺, found: 368.40; Anal. calcd for C₂₁H₂₂FN₃O₂: C 68.65, H 6.04, N 11.44, found: C 68.39, H 6.05, N 11.42.

4.1.5. (S)-1-(4-Fluorophenyl)-2-(1*H*-imidazol-1-yl)ethyl-4-(furan-2-carbonyl)piperazine-1-carboxylate [(S)-5a]:

(S)-1-(4-fluorophenyl)-2-(1*H*-imidazol-1-yl)ethanol (206 mg, 1 mmol) was suspended in 5 mL of dry CH₃CN, then triphosgene (148 mg, 0.5 mmol) was added. The mixture was stirred overnight at RT. After the obtained mixture was treated with Et₂O until the complete precipitation of a white precipitate. Subsequently the solvent was decanted off, the precipitate was suspended in dry CH₃CN and added with TEA (278 μL, 2.0 mmol), then with 1-(2-furoyl)piperazine (144 mg, 0.8 mmol). After 12 h at RT, the solvent was removed under reduced pressure, the obtained residue was treated with CH₂Cl₂ (10 mL) and extracted with saturated aqueous Na₂CO₃. The organic layer dried over Na₂SO₄ and evaporated under *vacuum* give a crude residue which was purified by silica gel column chromatography (CH₂Cl₂ / MeOH 80:20) resulting in (S)-5a as a waxy solid (257 mg, 78%, e.e. > 99%); IR (neat, ν cm⁻¹): 1699, 1621 (C=O); ¹H NMR (400 MHz, CD₃OD) δ (ppm): 3.50-3.79 (m, 8H), 4.42-4.49 (m, 2H), 5.99 (t, *J* = 6.0 Hz, 1H), 6.61 (s, 1H), 6.97 (s, 1H), 7.08-7.14 (m, 5H), 7.38-7.41 (m, 2H), 7.71 (s, 1H); ¹³C NMR (100 MHz, CD₃OD) δ (ppm): 52.5, 55.3, 73.5, 76.8, 112.5, 116.5 (*J* = 22.0 Hz), 118.0, 121.5, 129.0, 129.6 (*J* = 8.0 Hz), 134.7 (*J* = 3.0 Hz), 139.2, 146.1, 148.2, 155.3, 161.2, 164.2 (*J* = 244.0 Hz); MS (ESI): *m/z* calcd for C₂₁H₂₁FN₄O₄ 413.16 [M+H]⁺, found: 412.99; Anal. calcd for C₂₁H₂₁FN₄O₄: C 61.16, H 5.13, N 13.59, found: C 61.39, H 5.14, N 13.42.

4.1.6. (S)-1-(4-Chlorophenyl)-2-(1*H*-imidazol-1-yl)ethyl-4-(furan-2-carbonyl)piperazine-1-carboxylate [(S)-5b]:

According to the procedure described for (S)-5a, (S)-1-(4-chlorophenyl)-2-(1*H*-imidazol-1-yl)ethanol (111 mg, 0.5 mmol) was treated overnight with triphosgene (74 mg, 0.25 mmol), then TEA (139 μL, 1.0 mmol) and 1-(2-furoyl)piperazine (72 mg, 0.4 mmol) were added. The residue was purified by silica gel column chromatography using CH₂Cl₂ / MeOH 80:20

as eluent to obtain (S)-**5b** as a waxy solid (103 mg, 60 %, e.e. > 99%); IR (neat, ν cm^{-1}): 1701, 1622 (C=O); ^1H NMR (400 MHz, CDCl_3) δ (ppm): 3.09 (m, 4H), 3.64 (m, 4H), 4.30 (m, 2H), 5.92 (t, $J = 6.0$ Hz, 1H), 6.75 (s, 1H), 6.82 (d, $J = 8.3$ Hz, 2H), 7.03 (m, 2H), 7.15-7.22 (m, 4H), 7.31 (s, 1H); ^{13}C NMR (100 MHz, $\text{DMSO-}d_6$) δ (ppm): 43.9, 43.9, 52.6, 74.3, 111.8, 116.4, 121.4, 122.9, 128.6, 129.1, 133.6, 136.4, 136.7, 145.4, 147.2, 153.3, 158.9; MS (ESI): m/z calcd for $\text{C}_{21}\text{H}_{21}\text{ClN}_4\text{O}_4$ 429.13 $[\text{M}+\text{H}]^+$, found: 428.98; Anal. calcd for $\text{C}_{21}\text{H}_{21}\text{ClN}_4\text{O}_4$: C 58.81, H 4.94, N 13.06, found: C 58.49, H 4.96, N 13.24.

4.1.7. (S)-1-(4-fluorophenyl)-2-(1*H*-imidazol-1-yl)ethyl-4-(4-nitrophenyl)piperazine-1-carboxylate [(S)-**5c**]:

According to the procedure described for (S)-**5a**, (S)-1-(4-fluorophenyl)-2-(1*H*-imidazol-1-yl)ethanol (103 mg, 0.5 mmol) was treated overnight with triphosgene (74 mg, 0.25 mmol), then TEA (139 μL , 1.0 mmol) and 1-(4-nitrophenyl)piperazine (83 mg, 0.4 mmol) were added. The residue was purified by silica gel column chromatography using CH_2Cl_2 / MeOH 80:20 to obtain (S)-**5c** as a yellow solid (123 mg, 70 %, e.e. > 99%); mp: 168-169 $^\circ\text{C}$; IR (neat, ν cm^{-1}): 1704 (C=O); ^1H NMR (400 MHz, CDCl_3) δ (ppm): 3.45 (m, 4H), 3.70 (m, 4H), 4.42 (m, 2H), 6.00 (t, $J = 5.2$ Hz, 1H), 6.83 (m, 3H), 7.09 (m, 3H), 7.24 (m, 2H), 7.87 (s, 1H), 8.16 (d, $J = 8.9$ Hz, 2H); ^{13}C NMR (100 MHz, CDCl_3) δ (ppm): 46.8, 52.1, 74.9, 77.2, 113.2, 116.1 ($J = 22.0$ Hz), 119.8, 125.9, 128.0 ($J = 8.0$ Hz), 128.2, 132.4 ($J = 3.0$ Hz), 137.5, 139.3, 153.5, 154.4, 162.9 ($J = 247.0$ Hz); MS (ESI): m/z calcd for $\text{C}_{22}\text{H}_{22}\text{FN}_5\text{O}_4$ 440.17 $[\text{M}+\text{H}]^+$, found: 439.93; Anal. calcd for $\text{C}_{21}\text{H}_{21}\text{ClN}_4\text{O}_4$: C 60.13, H 5.05, N 15.94, found: C 60.31, H 5.06, N 15.99.

4.1.8. (\pm)-1-(4-chlorophenyl)-2-(1*H*-imidazol-1-yl)ethyl-4-(4-nitrophenyl)piperazine-1-carboxylate (**5d**):

According to the procedure described for (S)-**5a**, (\pm)-1-(4-chlorophenyl)-2-(1*H*-imidazol-1-yl)ethanol (111 mg, 0.5 mmol) was treated with triphosgene (111 mg, 0.5 mmol); then TEA

(139 μ L, 1.0 mmol) and 1-(4-nitrophenyl)piperazine (83 mg, 0.4 mmol) were added. The residue was purified by silica gel column chromatography using CH_2Cl_2 / MeOH 80:20 as eluent to obtain **5d** as a yellow solid (146 mg, 80 %); mp: 188-190 $^\circ\text{C}$; IR (neat, ν cm^{-1}): 1704 (C=O); ^1H NMR (400 MHz, CDCl_3) δ (ppm): 3.42 (m, 4H), 3.68 (m, 4H), 4.33 (m, 2H), 5.94 (t, J = 5.5 Hz, 1H), 6.81 (m, 3H), 7.04 (s, 1H), 7.14 (d, J = 10.5 Hz, 2H), 7.34 (m, 2H), 7.45 (s, 1H), 8.14 (d, J = 9.3 Hz, 2H); ^{13}C NMR (100 MHz, CDCl_3) δ (ppm): 43.3, 46.8, 51.7, 75.0, 113.1, 119.7, 125.9, 127.5, 129.1, 129.2, 135.0, 135.2, 137.6, 139.2, 153.5, 154.4; MS (ESI): m/z calcd for $\text{C}_{22}\text{H}_{22}\text{ClN}_5\text{O}_4$ 456.14 $[\text{M}+\text{H}]^+$, found: 455.97; Anal. calcd for $\text{C}_{22}\text{H}_{22}\text{ClN}_5\text{O}_4$: C 57.96, H 4.86, N 15.36, found: C 58.18, H 4.85, N 15.41.

4.1.9. (S)-1-(4-Fluorophenyl)-2-(1*H*-imidazol-1-yl)ethyl-4-(4-chlorophenyl)piperazine-1-carboxylate [(S)-5e]:

According to the procedure described for (S)-**5a**, (S)-1-(4-fluorophenyl)-2-(1*H*-imidazol-1-yl)ethanol (103 mg, 0.5 mmol) was treated with triphosgene (74 mg, 0.25 mmol); then TEA (139 μ L, 1.0 mmol) and 1-(4-chlorophenyl)piperazine (78 mg, 0.4 mmol) were added. The residue was purified by silica gel column chromatography using CH_2Cl_2 / MeOH 80:20 as eluent to obtain (S)-**5e** as a waxy solid (158 mg, 92 %, e.e. > 99%); IR (neat, ν cm^{-1}): 1703 (C=O); ^1H NMR (400 MHz, $\text{DMSO}-d_6$) δ (ppm): 3.04 (m, 4H), 3.38 (m, 4H), 4.36 (m, 2H), 5.83 (m, 1H), 6.84 (s, 1H), 6.95 (d, J = 8.9 Hz, 2H), 7.13-7.24 (m, 5H), 7.38 (dd, J = 7.8, 5.5 Hz, 2H), 7.56 (s, 1H); ^{13}C NMR (100 MHz, $\text{DMSO}-d_6$) δ (ppm): 43.2, 48.1, 50.5, 74.7, 115.3 (J = 22 Hz), 117.5, 120.1, 123.0, 128.1, 128.4 (J = 9 Hz), 128.7, 133.9 (J = 2 Hz), 137.8, 149.5, 153.2, 161.8 (J = 243 Hz); MS (ESI): m/z calcd for $\text{C}_{22}\text{H}_{22}\text{ClFN}_4\text{O}_2$ 429.15 $[\text{M}+\text{H}]^+$, found: 428.89; Anal. calcd for $\text{C}_{22}\text{H}_{22}\text{ClFN}_4\text{O}_2$: C 61.61, H 5.17, N 13.06, found: C 61.41, H 5.16, N 13.12.

4.1.10. (S)-1-(4-Chlorophenyl)-2-(1*H*-imidazol-1-yl)ethyl-4-(4-chlorophenyl)piperazine-1-carboxylate [(S)-5f]:

According to the procedure described for (S)-**5a**, (S)-1-(4-chlorophenyl)-2-(1*H*-imidazol-1-yl)ethanol (113 mg, 0.5 mmol) was treated with triphosgene (74 mg, 0.25 mmol); then TEA (13.9 μ L, 1.0 mmol) and 1-(4-chlorophenyl)piperazine (78 mg, 0.4 mmol) were added. The residue was purified by silica gel column chromatography using CH_2Cl_2 / MeOH 80:20 as eluent to obtain (S)-**5f** as a white solid (157 mg, 88 %, e.e. > 99%); mp: 113-116 $^\circ\text{C}$; IR (neat, ν cm^{-1}): 1702 (C=O); ^1H NMR (400 MHz, $\text{DMSO-}d_6$) δ (ppm): 3.09 (m, 4H), 3.65 (m, 4H), 4.38 (m, 2H), 5.88 (m, 1H), 6.84 (s, 1H), 6.97 (d, $J = 8.9$ Hz, 2H), 7.13 (s, 1H), 7.25 (d, $J = 8.9$ Hz, 2H), 7.37 (d, $J = 8.3$ Hz, 2H), 7.45 (d, $J = 8.3$ Hz, 2H), 7.53 (s, 1H); ^{13}C NMR (100 MHz, CD_3OD) δ (ppm): 43.4, 48.9, 51.1, 75.1, 117.7, 120.1, 124.7, 127.4, 127.7, 128.2, 128.7, 134.1, 136.2, 137.8, 149.9, 153.8; MS (ESI): m/z calcd for $\text{C}_{22}\text{H}_{22}\text{Cl}_2\text{N}_4\text{O}_2$ 445.12 $[\text{M}+\text{H}]^+$, found: 444.87; Anal. calcd for $\text{C}_{22}\text{H}_{22}\text{Cl}_2\text{N}_4\text{O}_2$: C 59.33, H 4.98, N 12.58, found: C 59.09, H 4.99, N 12.52.

4.1.11. (S)-2-(1*H*-imidazol-1-yl)-1-phenylethyl-4-(3,4-dichlorophenyl)piperazine-1-carboxylate [(S)-5g**]:**

According to the procedure described for (S)-**5a**, (S)-2-(1*H*-imidazol-1-yl)-1-phenylethanol (300 mg, 1.6 mmol) in 15 mL of dry CH_3CN was treated with triphosgene (236 mg, 0.8 mmol); then TEA (442 μ L, 3.2 mmol) and 1-(3,4-dichlorophenyl)piperazine (293 mg, 1.3 mmol) were added. The residue was purified by silica gel column chromatography using EtOAc / MeOH 90:10 as eluent; the obtained waxy residue was triturated with Et_2O to give a white solid (48 mg, 27 %, e.e. > 99%); mp: 118-120 $^\circ\text{C}$; IR (neat, ν cm^{-1}): 1700 (C=O); ^1H NMR (400 MHz, $\text{DMSO-}d_6$) δ (ppm): 3.15 (m, 4H), 3.64 (m, 4H), 4.38 (m, 2H), 5.88 (m, 1H), 6.85 (s, 1H), 6.96 (dd, $J = 8.8, 2.8$ Hz, 1H), 7.14 (s, 1H), 7.16 (d, $J = 2.8$ Hz, 2H), 7.33-7.43 (m, 5H), 7.55 (s, 1H); ^{13}C NMR (50 MHz, Acetone- d_6) δ (ppm): 43.3, 48.1, 51.2, 75.6, 116.0, 117.2, 119.7, 121.2, 126.3, 128.2, 128.5, 130.5, 132.1, 137.9, 138.2, 151.1,

153.5; MS (ESI): m/z calcd for $C_{22}H_{22}Cl_2N_4O_2$ 445.12 $[M+H]^+$, found: 445.00; Anal. calcd for $C_{22}H_{22}Cl_2N_4O_2$: C 59.33, H 4.98, N 12.58, found: C 59.55, H 4.99, N 12.61.

4.1.12. (S)-1-(4-Fluorophenyl)-2-(1*H*-imidazol-1-yl)ethyl-4-(3,4-dichlorophenyl)piperazine-1-carboxylate [(S)-5h]:

According to the procedure described for (S)-5a, (S)-1-(4-fluorophenyl)-2-(1*H*-imidazol-1-yl)ethanol (103 mg, 0.5 mmol) was treated with triphosgene (72 mg, 0.25 mmol); then TEA (139 μ L, 1.0 mmol) and 1-(3,4-dichlorophenyl)piperazine (92 mg, 0.4 mmol) were added. The residue was purified by silica gel column chromatography using CH_2Cl_2 / MeOH 90:10 as eluent; the obtained waxy residue was triturated with Et_2O to give a white solid (111 mg, 60 %, e.e. > 99%); mp: 134-135 $^{\circ}C$; IR (neat, ν cm^{-1}): 1700 (C=O); 1H NMR (400 MHz, $CDCl_3$) δ (ppm): 3.15 (m, 4H), 3.66 (m, 4H), 4.32 (m, 2H), 5.95 (t, J = 5.2 Hz, 1H), 6.75 (m, 2H), 6.98 (d, J = 2.8 Hz, 1H), 7.05 (m, 3H), 7.18 (m, 2H), 7.32 (m, 2H); ^{13}C NMR (100 MHz, $CDCl_3$) δ (ppm): 43.6, 48.8, 51.8, 74.9, 115.9 (J = 21 Hz), 116.0, 118.0, 119.6, 123.2, 127.9 (J = 8 Hz), 129.5, 130.6, 132.7 (J = 2 Hz), 132.9, 137.7, 150.3, 153.6, 162.8 (J = 247 Hz); MS (ESI): m/z calcd for $C_{22}H_{21}Cl_2FN_4O_2$ 463.11 $[M+H]^+$, found: 463.00; Anal. calcd for $C_{22}H_{21}Cl_2FN_4O_2$: C 57.03, H 4.57, N 12.09, found: C 57.23, H 4.57, N 12.12.

4.1.13. (\pm)-1-(4-Chlorophenyl)-2-(1*H*-imidazol-1-yl)ethyl-4-(3,4-dichlorophenyl)piperazine-1-carboxylate (5i):

According to the procedure described for (S)-5a, (\pm)-1-(4-chlorophenyl)-2-(1*H*-imidazol-1-yl)ethanol (100 mg, 0.45 mmol) was treated with triphosgene (74 mg, 0.25 mmol); then TEA (125 μ L, 0.9 mmol) and 1-(3,4-dichlorophenyl)piperazine (83 mg, 0.36 mmol) were added. The residue was purified by silica gel column chromatography using EtOAc / MeOH 95:5 as eluent; the obtained waxy residue was triturated with Et_2O to give a white solid (52 mg, 30 %); mp: 143-145 $^{\circ}C$; IR (neat, ν cm^{-1}): 1702 (C=O); 1H NMR (400 MHz, CD_3OD) δ (ppm): 3.16 (m, 4H), 3.57-3.74 (m, 4H), 4.46 (d, J = 5.8 Hz, 2H), 5.98 (t, J = 5.8

Hz, 1H), 6.92 (dd, $J = 8.9, 2.8$ Hz, 1H), 6.96 (s, 1H), 7.11 (d, $J = 2.8$ Hz, 1H), 7.13 (s, 1H), 7.34-7.41 (m, 5H), 7.58 (s, 1H); ^{13}C NMR (100 MHz, Acetone- d_6) δ (ppm): 43.3, 48.1, 51.0, 75.1, 116.1, 117.2, 120.2, 121.2, 128.0, 128.2, 128.6, 130.6, 132.1, 133.6, 136.8, 138.1, 151.0, 153.7; MS (ESI): m/z calcd for $\text{C}_{22}\text{H}_{21}\text{Cl}_3\text{N}_4\text{O}_2$ 479.08 $[\text{M}+\text{H}]^+$, found: 479.08; Anal. calcd for $\text{C}_{22}\text{H}_{21}\text{Cl}_3\text{N}_4\text{O}_2$: C 55.07, H 4.41, N 11.68, found: C 55.27, H 4.40, N 11.70.

4.1.14. (S)-1-(2,4-Dichlorophenyl)-2-(1H-imidazol-1-yl)ethyl-4-(3,4-dichlorophenyl)piperazine-1-carboxylate [(S)-5l]:

According to the procedure described for (S)-5a, (S)-1-(2,4-dichlorophenyl)-2-(1H-imidazol-1-yl)ethanol (100 mg, 0.4 mmol) was treated with triphosgene (59 mg, 0.2 mmol); then TEA (111 μL , 0.8 mmol) and 1-(3,4-dichlorophenyl)piperazine (74 mg, 0.32 mmol) were added. The residue was purified by silica gel column chromatography using CH_2Cl_2 / MeOH 95:5 as eluent to obtain a white solid (113 mg, 61 %); mp: 61-63 $^\circ\text{C}$; IR (neat, ν cm^{-1}): 1707 (C=O); ^1H NMR (400 MHz, CDCl_3) δ (ppm): 3.15 (m, 4H), 3.65 (m, 4H), 4.29 (dd, $J = 14.9, 6.1$ Hz, 1H), 4.43 (dd, $J = 14.9, 3.5$ Hz, 1H), 6.29 (dd, $J = 6.0, 2.2$ Hz, 1H), 6.72-6.76 (m, 2H), 6.94-6.98 (m, 2H), 7.02 (s, 1H), 7.21 (dd, $J = 8.3, 2.0$ Hz, 1H), 7.30-7.34 (m, 2H), 7.45 (d, $J = 2.0$ Hz, 1H); ^{13}C NMR (100 MHz, CDCl_3) δ (ppm): 43.7, 48.8, 49.7, 72.4, 116.0, 118.0, 119.7, 123.3, 127.8, 127.9, 129.5, 129.8, 130.6, 132.4, 132.9, 133.2, 135.2, 137.7, 150.2, 153.1; MS (ESI): m/z calcd for $\text{C}_{22}\text{H}_{20}\text{Cl}_4\text{N}_4\text{O}_2$ 513.04 $[\text{M}+\text{H}]^+$, found: 514.73; Anal. calcd for $\text{C}_{22}\text{H}_{20}\text{Cl}_4\text{N}_4\text{O}_2$: C 51.38, H 3.92, N 10.90, found: C 51.39, H 3.91, N 10.95.

4.1.15. (S)-2-(1H-imidazol-1-yl)-1-(4-nitrophenyl)ethyl-4-(3,4-dichlorophenyl)piperazine-1-carboxylate [(S)-5m]:

According to the procedure described for (S)-5a, (S)-1-(4-nitrophenyl)-2-(1H-imidazol-1-yl)ethanol (**50**) (130 mg, 0.56 mmol) was treated with triphosgene (83 mg, 0.28 mmol); then TEA (156 μL , 1.12 mmol) and 1-(3,4-dichlorophenyl)piperazine (104 mg, 0.45 mmol) were added. The residue was purified by silica gel column chromatography using CH_2Cl_2 / MeOH / n -

hexane 90:10:10 as eluent to obtain a yellow solid (55 mg, 25 %); mp:163-165°C (Kofler apparatus); IR (neat, ν cm^{-1}): 1707 (C=O); ^1H NMR (400 MHz, CDCl_3) δ (ppm): 3.16 (m, 4H), 3.63-3.71 (m, 4H), 4.39 (dd, J = 14.6, 6.1 Hz, 1H), 4.42 (dd, J = 14.6, 4.6 Hz, 1H), 6.06 (m, 1H), 6.77 (m, 2H), 6.98 (d, J = 2.7 Hz, 1H), 7.05 (s, 1H), 7.28-7.38 (m, 4H), 8.24 (d, J = 6.85 Hz, 2H); ^{13}C NMR (100 MHz, CDCl_3) δ (ppm): 43.6, 48.9, 51.4, 74.6, 116.1, 118.1, 119.5, 123.5, 124.2, 127.0, 129.8, 130.7, 133.0, 137.7, 144.0, 148.1, 150.2, 153.2; MS (ESI): m/z calcd for $\text{C}_{22}\text{H}_{21}\text{Cl}_2\text{N}_5\text{O}_4$ 490.10 $[\text{M}+\text{H}]^+$, found: 489.53; Anal. calcd for $\text{C}_{22}\text{H}_{21}\text{Cl}_2\text{N}_5\text{O}_4$: C 53.89, H 4.32, N 14.28, found: C 53.77, H 4.33, N 14.23.

4.1.16 (S)-1-([1,1'-biphenyl]-4-yl)-2-(1*H*-imidazol-1-yl)ethyl-4-(3,4-dichlorophenyl)piperazine-1-carboxylate [(S)-5n]:

1-(3,4-Dichlorophenyl)piperazine (173 mg, 0.75 mmol) in CH_2Cl_2 (1 mL) was added dropwise to a solution of triphosgene (83mg, 0.28 mmol) and pyridine (130 μL , 1.61 mmol) in CH_2Cl_2 (2 mL). After 3 h at RT, the mixture was diluted with CH_2Cl_2 (5 mL), then the corresponding solution was washed with H_2O (2x5mL). The organic layer dried over Na_2SO_4 and evaporated under *vacuum* to give a yellow oil used without further purification, dissolved in CH_2Cl_2 (5 mL) and added to a solution of (S)-1-(biphenyl-4-yl)-2-(1*H*-imidazol-1-yl)ethanol (**51**) (100 mg, 0.38 mmol), TEA (47 μL , 0.41 mmol) and DMAP (20 % mmol). From the suspension resulting after 12 h at RT the solid was removed by filtration; the obtained filtrate was diluted with CH_2Cl_2 and washed with saturated aqueous NaHCO_3 . The organic layer, dried under Na_2SO_4 , was evaporated under reduced pressure and was purified by silica gel column chromatography (CH_2Cl_2 / MeOH 90:10) to give solid yellow. Further purification was carried out by semipreparative HPLC on a Lichrosorb RP-18(5 μm) column, 250-10 mm. $\lambda=254\text{nm}$ (elution profile: MeOH: H_2O 90:10, 2.0 mL/min) to give a white solid (25 mg, 16%); mp: 74-75°C; IR (neat, ν cm^{-1}): 1702 (C=O); ^1H NMR (400 MHz, $\text{DMSO}-d_6$) δ (ppm): 3.16 (m, 4H), 3.66 (m, 4H), 4.38-4.49 (m, 2H), 5.92 (m, 1H), 6.88 (s,

1H), 6.96 (dd, $J = 6.4, 2.8$ Hz, 1H), 7.17 (d, $J = 2.8$ Hz, 1H), 7.20 (s, 1H), 7.41-7.48 (m, 6H), 7.67 (s, 1H), 7.69 (m, 4H); ^{13}C NMR (100 MHz, CDCl_3) δ (ppm): 43.6, 48.9, 51.9, 75.4, 116.0, 118.0, 122.8, 123.2, 123.6, 126.6, 127.1, 127.7, 128.9, 130.6, 133.0, 135.8, 140.3, 141.9, 150.3, 153.7; MS (ESI): m/z calcd for $\text{C}_{28}\text{H}_{26}\text{Cl}_2\text{N}_4\text{O}_2$ 521.15 $[\text{M}+\text{H}]^+$, found: 520.80; Anal. calcd for $\text{C}_{28}\text{H}_{26}\text{Cl}_2\text{N}_4\text{O}_2$: C 64.49, H 5.03, N 10.74, found: C 64.91, H 5.02, N 10.70.

4.1.17. (S)-2-(1H-imidazol-1-yl)-1-(naphthalen-1-yl)ethyl-4-(3,4-dichlorophenyl)piperazine-1-carboxylate [(S)-6]:

According to the procedure described for (S)-5a, (S)-1-(naphthalen-1-yl)-2-(1H-imidazol-1-yl)ethanol (**52**) (100 mg, 0.42 mmol) was activated with triphosgene (62 mg, 0.28 mmol); then TEA (117 μL , 0.84 mmol) and 1-(3,4-dichlorophenyl)piperazine (76 mg, 0.34 mmol) were added. After silica gel column chromatography (CH_2Cl_2 / MeOH 90:10) the fractions with $R_f = 0.65$ were collected and purified by a further silica gel column chromatography on silica gel using CH_3CN / CH_2Cl_2 50:50 as eluent; the fractions with $R_f = 0.43$ were collected to furnish a white solid, subsequently crystallized from EtOAc (34 mg, 20 %); mp: 152-154°C (Kofler apparatus); IR (neat, ν cm^{-1}): 1707 (C=O); ^1H NMR (400 MHz, CDCl_3) δ (ppm): 3.15 (m, 4H), 3.62-3.73 (m, 4H), 4.43 (m, 2H), 6.13 (t, $J = 5.6$ Hz, 1H), 6.75 (dd, $J = 9.2, 2.8$ Hz, 1H), 6.80 (s, 1H), 6.98 (d, $J = 2.8$ Hz, 1H), 7.03 (s, 1H), 7.31 (s, 1H), 7.33 (s, 1H), 7.36 (s, 1H), 7.52-7.54 (m, 2H), 7.69 (s, 1H), 7.81-7.88 (m, 3H); ^{13}C NMR (100 MHz, CDCl_3) δ (ppm): 43.5, 48.9, 51.8, 75.8, 116.0, 118.0, 119.7, 123.3, 125.8, 126.7, 127.8, 128.1, 128.9, 129.5, 130.6, 133.0, 133.1, 133.4, 134.2, 136.8, 137.8, 150.3, 153.7, 156.0; MS (ESI): m/z calcd for $\text{C}_{26}\text{H}_{24}\text{Cl}_2\text{N}_4\text{O}_2$ 495.13 $[\text{M}+\text{H}]^+$, found: 494.47; Anal. calcd for $\text{C}_{26}\text{H}_{24}\text{Cl}_2\text{N}_4\text{O}_2$: C 63.04, H 4.88, N 11.31, found: C 63.14, H 4.89, N 11.35.

4.1.18. (S)-1-(4-chlorophenyl)-2-(1H-imidazol-1-yl)ethyl-4-((4-nitrophenyl)thio)phenyl)carbamate [(S)-7]:

According to the procedure described for (S)-**5a**, (S)-1-(4-chlorophenyl)-2-(1*H*-imidazol-1-yl)ethanol (222 mg, 1.0 mmol) was treated with triphosgene (148 mg, 0.5 mmol) in dry CH₃CN (5 mL); then TEA (417 μ L, 3.0 mmol) and 4-((4-nitrophenyl)thio)aniline (197 mg, 0.8 mmol) were added. The residue was purified by silica gel column chromatography using CHCl₃ / MeOH 90:10 as eluent to obtain a yellow solid (336 mg, 85 %, e.e. > 98%); mp: 100-102 $^{\circ}$ C; IR (neat, ν cm⁻¹): 1727 (C=O); ¹H NMR (400 MHz, CD₃OD) δ (ppm): 4.49 (m, 2H), 6.04 (t, *J* = 6.2 Hz, 1H), 6.96 (s, 1H), 7.18 (m, 3H), 7.38 (m, 4H), 7.49 (d, *J* = 8.8 Hz, 2H), 7.57 (m, 3H), 8.08 (d, *J* = 9.05 Hz, 2H); ¹³C NMR (100 MHz, DMSO-*d*₆) δ (ppm): 50.7, 74.6, 120.2, 120.6, 122.2, 124.7, 126.5, 128.6, 128.7, 129.0, 133.4, 136.5, 137.1, 138.4, 141.1, 145.3, 149.2, 152.6; MS (ESI): *m/z* calcd for C₂₄H₁₉ClN₄O₄S 495.09 [M+H]⁺, found: 495.07; Anal. calcd for C₂₄H₁₉ClN₄O₄S: C 58.24, H 3.87, N 11.32, found: C 58.34, H 3.88, N 11.33.

4.1.19. (\pm)-1-(4-chlorophenyl)-2-phenylethyl-4-(3,4-dichlorophenyl)piperazine-1-carboxylate (**8**):

1-(3,4-Dichlorophenyl)piperazine (173 mg, 0.75 mmol) in CH₂Cl₂ (1 mL) was added dropwise to a solution of triphosgene (83 mg, 0.28 mmol) and pyridine (130 μ L, 1.61 mmol) in CH₂Cl₂ (2 mL). After 3 h at RT, the mixture was diluted with CH₂Cl₂ (5 mL), then the corresponding solution was washed with H₂O (2x5 mL). The organic layer dried over Na₂SO₄ and evaporated under *vacuum* to give a yellow oil used without further purification, dissolved in CH₂Cl₂ (5 mL) and added to a solution of 1-(4-chlorophenyl)-2-phenylethanol (**53**) (120 mg, 0.5 mmol), TEA (83 μ L, 0.6 mmol) and DMAP (20 % mmol). The reaction mixture was stirred overnight at RT. The corresponding orange suspension was diluted with CH₂Cl₂ (5 mL) and washed with saturated aqueous NaHCO₃. The organic layer, dried under Na₂SO₄, was evaporated under reduced pressure. The crude product was purified by silica gel column chromatography (CH₂Cl₂ / MeOH 95:5) to give **8** as a waxy solid (35

mg, 15%); IR (neat, ν cm^{-1}): 1698 (C=O); ^1H NMR (400 MHz, CD_3Cl) δ (ppm): 3.07-3.25 (m, 6H), 3.53-3.71 (m, 4H), 5.92 (m, 1H), 6.96 (dd, $J = 8.9, 2.8$ Hz, 1H), 7.12 (d, $J = 2.8$ Hz, 1H), 7.19-7.30 (m, 5H), 7.38-7.41 (m, 5H); ^{13}C NMR (100 MHz, Acetone- d_6) δ (ppm): 42.2, 42.9, 47.7, 76.2, 115.5, 116.7, 120.7, 125.9, 127.6, 127.7, 129.1, 130.0, 131.6, 132.3, 136.9, 139.7, 150.6, 153.3, 165.2; MS (ESI): m/z calcd for $\text{C}_{25}\text{H}_{23}\text{Cl}_3\text{N}_2\text{O}_2$ 489.09 $[\text{M}+\text{H}]^+$, found: 490.60; Anal. calcd for $\text{C}_{25}\text{H}_{23}\text{Cl}_3\text{N}_2\text{O}_2$: C 61.30, H 4.73, N 5.72, found: C 61.34, H 4.72, N 5.78.

4.1.20. (\pm)-1-(4-chlorophenyl)-2-(1*H*-pyrrol-1-yl)ethyl-4-(3,4-dichlorophenyl)piperazine-1-carboxylate (9**):**

(\pm)-1-(4-Chlorophenyl)-2-(1*H*-pyrrol-1-yl)ethanol (**54**) (60 mg, 0.27 mmol) was used to prepare **9** according to the procedure described for **8**. The residue was purified by silica gel column chromatography using CH_2Cl_2 / MeOH / *n*-hexane 95:5:5 as eluent to obtain a waxy solid (45 mg, 35 %); IR (neat, ν cm^{-1}): 1698 (C=O); ^1H NMR (400 MHz, CD_3OD) δ (ppm): 3.16 (m, 4H), 3.56-3.74 (m, 4H), 4.29 (m, 2H), 5.99 (m, 1H), 6.02 (m, 2H), 6.64 (m, 2H), 6.92 (dd, $J = 8.9, 2.9$ Hz, 1H), 7.11 (d, $J = 2.9$ Hz, 1H), 7.28-7.37 (m, 5H); ^{13}C NMR (100 MHz, Acetone- d_6) δ (ppm): 43.5, 48.2, 53.8, 75.7, 107.9, 116.0, 117.2, 121.2, 121.3, 128.1, 128.4, 130.5, 132.2, 133.3, 137.7, 151.1, 153.5; MS (ESI): m/z calcd for $\text{C}_{23}\text{H}_{22}\text{Cl}_3\text{N}_3\text{O}_2$ 478.08 $[\text{M}+\text{H}]^+$, found: 479.67; Anal. calcd for $\text{C}_{23}\text{H}_{22}\text{Cl}_3\text{N}_3\text{O}_2$: C 57.70, H 4.63, N 8.78, found: C 57.80, H 4.64, N 8.75.

4.1.21. (*S*)-2-(1*H*-imidazol-1-yl)-1-(4-nitrophenyl)ethanol (50**):**

A Schlenk tube was charged with CH_2Cl_2 (6 mL), TEA (225 μL , 1.62 mmol), 2-(1*H*-imidazol-1-yl)-1-(4-nitrophenyl)ethanone (75 mg, 0.32 mmol) and [(*R,R*)-TsDPEN Ru-(Cymene)Cl (0.1% mol) under N_2 flow and then HCOOH (526 μL , 12.8 mmol) was added over a period of an hour via GC-syringe. During the addition, the temperature rose slowly to 30°C. The mixture was heated at 40°C for 26 h. The solvent volume was reduced

approximately to 3 mL, the solid was recovered, washed with CH₂Cl₂ (2x2 mL) and crystallized with EtOH to give a yellow solid (45 mg, 60 %, e.e. > 99%). ¹H NMR (400 MHz, DMSO-*d*₆) δ (ppm): 4.11 (m, 2H), 5.01 (m, 1H), 6.07 (s br, 1H, D₂O exchange), 6.83 (s, 1H), 7.10 (s, 1H), 7.48 (s, 1H), 7.61 (d, *J* = 7.7 Hz, 2H), 8.19 (d, *J* = 7.7 Hz, 2H).

4.1.22. (S)-1-(biphenyl-4-yl)-2-(1*H*-imidazol-1-yl)ethanol (51):

A Schlenk tube was charged with CH₂Cl₂ (7.0 mL), TEA (530 μL, 3.8 mmol), 1-(biphenyl-4-yl)-2-(1*H*-imidazol-1-yl)ethanone (200 mg, 0.76 mmol) and [(*R,R*)-TsDPEN Ru-(Cymene)Cl (0.1 % mol) under N₂ flow and then HCOOH (157 μL, 3.8 mmol) was added over a period of an hour via GC-syringe. During the addition, the temperature rose slowly to 30°C. The mixture was heated at 40°C for 26 h, to give a suspension. The solid was recovered and purified by silica gel column chromatography using CHCl₃ / MeOH / *n*-hexane 90:10:5 as eluent to obtain a white solid subsequently crystallized from EtOH (83 mg, 41 %, e.e. > 99%). ¹H NMR (400 MHz, DMSO-*d*₆) δ (ppm): 4.07 (dd, *J* = 14.0, 7.9 Hz, 1H), 4.18 (dd, *J* = 14.0, 4.0 Hz, 1H), 4.86 (m, 1H), 5.78 (s br, 1H, D₂O exchange), 6.85 (s, 1H), 7.16 (s, 1H), 7.36 (t, *J* = 7.3 Hz, 1H), 7.43-7.48 (m, 4H), 7.55 (s, 1H), 7.63-7.67 (m, 4H).

4.1.23. (S)-2-(1*H*-imidazol-1-yl)-1-(naphthalen-1-yl)ethanol (52):

(S)-2-(1*H*-imidazol-1-yl)-1-(naphthalen-1-yl)ethanol (**52**) was prepared in according to the procedure described for **50**, to give a white solid crystallized from EtOAc (55 %, e.e. > 99%). ¹H NMR (400 MHz, DMSO-*d*₆) δ (ppm): 4.14 (dd, *J* = 13.9, 7.8 Hz, 1H), 4.25 (dd, *J* = 13.9, 4.0 Hz, 1H), 4.99 (m, 1H), 5.87 (s br, 1H, D₂O exchange), 6.82 (s, 1H), 7.14 (s, 1H), 7.49-7.54 (m, 4H), 7.84-7.91 (m, 4H).

4.1.24. (±)-1-(4-Chlorophenyl)-2-phenylethanol (53):

Commercial 1-(4-chlorophenyl)-2-phenylethanone (2.0 g, 8.7 mmol) was solubilized in CH₂Cl₂ / MeOH 50:50 (400 mL), then NaBH₄ (0.8 g, 21.2 mmol) was added in small portions. After 24 h at RT the solvents were removed under reduced pressure; the crude mixture was neutralized with aqueous HCl 10% and extracted with EtOAc (2x25mL). The organic layers were dried over Na₂SO₄ and purified by silica gel column chromatography using EtOAc / *n*-hexane 20:80 to give a waxy solid (1.9 g, 94%); ¹H NMR (400 MHz, DMSO-*d*₆) δ (ppm): 2.87 (m, 2H), 4.76 (m, 1H), 5.38 (m, 1H, D₂O exchange), 7.35-7.13 (m, 9H).

4.1.25. (±)-1-(4-Chlorophenyl)-2-(1*H*-pyrrol-1-yl)ethanol (54):

To a solution of hexamethylenetetramine (1.8 g, 0.013 mol) in CH₂Cl₂ (70 mL) 2-bromo-1-(4-chlorophenyl)ethanone (3.0 g, 0.013 mol) was added in small portions. After 3 h at RT, the corresponding suspension was filtered; the obtained white solid was dried under reduced pressure and treated with EtOH (30 mL) and HCl 37 % (3.75 mL) for 3 days at RT. After this time, the suspension was filtered; the solvent was removed and the residue was washed with H₂O and dried over P₂O₅ to give a yellowish solid (550 mg). The solid was recovered with DMF (10 mL) and heated up to 150 °C, then 2,5-dimethoxytetrahydrofuran (394 μL, 3.04 mmol) was added. After 5 minutes, the mixture was poured into ice and left overnight at 4 °C. The resulting suspension was filtered and the solid was washed with H₂O and dried over P₂O₅ under reduced pressure to give a brownish solid (350 mg). It was used without further purification for the subsequent reduction with NaBH₄ (87mg, 2.3 mmol) in CH₂Cl₂ / MeOH 50:50 (40 mL) for 2 h at RT. Then, the solvents mixture was removed under reduced pressure; the crude mixture was neutralized with aqueous HCl 10% and extracted with CH₂Cl₂ (3x10mL). The combined organic layers were dried over Na₂SO₄ and evaporated, to yield a waxy solid (288 mg) used without further purification. ¹H NMR (400 MHz, DMSO-*d*₆) δ (ppm): 3.98 (m, 2H), 4.81

(m, 1H), 5.68 (d, $J = 4.6$ Hz, 1H, D₂O exchange), 5.92 (m, 2H), 6.66 (m, 2H), 7.30 (d, $J = 8.3$ Hz, 2H), 7.36 (d, $J = 8.3$ Hz, 2H).

4.2. Molecular modeling

4.2.1. Ligand conformational analysis. Ligand flexibility was taken into account by considering each compound as a collection of conformers representing different areas of the conformational space, which is accessible to the molecule within a given energy range. For each compound, conformers were generated using the CAESAR algorithm implemented in Discovery Studio 2.5.[38] Conformational ensembles were generated with an energy threshold of 25 kcal/mol from the locally minimized structure, and a maximum of 1000 conformers per molecule was allowed.

During the optimization of the 3-phenylpyrazolo[1-5a]pyrimidin-7(4H)-one, ligand conformational analysis was performed with Omega 2 from OpenEye. We left all the parameters of the Omega2 [36] program to the default values generating 792.744.404 conformers.

4.2.2. Generation of common features pharmacophore model and virtual screening.

The three-dimensional structures of 71 compounds in the training set (see Supporting Information) were imported into *Discovery Studio 2.5*, ACCELRYs.[38] During the generation of pharmacophoric hypotheses, the following chemical functions were selected in the feature dictionary of CATALYST: hydrogen bond acceptor, hydrogen bond acceptor lipid (*to include the basic nitrogen*), hydrogen bond donor, aromatic ring, positive ionizable, hydrophobic aromatic and hydrophobic aliphatic. The maximum number of pharmacophores generated by HipHop was set to 10, while the minimum number of features to be included in each pharmacophore was set to 4, having an interfeature distance of 2.97 Å (default value). *HipHop-REFINE* was used to refine the pharmacophoric

hypotheses by means of excluded volumes. The tool uses inactive compounds of the training set to place excluded volumes that resemble the steric constraints of the binding pocket. Maximum number of excluded volumes was set to 100. Pharmacophore screening was performed with Discovery Studio 2.5, by using default parameters.

4.2.3. Optimization of the 3-phenylpyrazolo[1-5a]pyrimidin-7(4H)-one scaffold. We chose the ZINC database [39] to perform the virtual screening. We selected the commercially available part of the database (“All Now”) composed of about 9.050.000 molecules. Filtration of compounds was performed with Filter (OpenEye).[32, 36] We left most of parameters of Filter to the default values. We changed the parameters controlling molecular weight, polarity, solubility, the presence of specific functional groups, tendency to aggregation of molecules and the values of the variables that control the oral bioavailability of the compounds (Table 4).[40] These modifications of the filter were applied keeping in mind that the target, *M tuberculosis*, has a very lipophilic and tough cell wall to be crossed. All the changes were, indeed, focused on selection of compounds able to permeate through the microorganism cell wall. After the Filter step, the database was reduced from 9.050.000 to 5.242.737 molecules, equal to 42% decrease.

[Table 4]

The query was generated using four molecules, our hit and three compounds from two articles in the literature, using the software vROCS.[31, 32] The query validation was performed on two database of increasing size.[33, 34] The first was the Mao’s one (about 30 molecules) and the second was the Ananthan database, enriched with the Mao database, for a total of about 100.000 molecules. We performed the virtual screening with the program ROCS. Using the multiconformers and the query previously generated setting a cutoff for the TanimotoCombo scoring function of 0.6. The cutoff was set to 0.6 to reduce the number of compounds selected, removing those that were not able to map our query in

terms of physicochemical features or in terms of shape satisfactory. We visually inspected the first 5000 of the 46409 molecules obtained. A set of 13 compounds was purchased for biological test.

4.3. Biology

Compounds were dissolved in DMSO (Sigma-Aldrich Co., St. Louis, MO, USA) at concentrations ranging between 2.5 and 10 mg/mL and stored at -20 °C until use. To avoid interference by the solvent, the maximum concentration of DMSO used in the assays was 1%.

4.3.1. Inhibition of *M. tuberculosis* growth. Minimum inhibitory concentrations (MICs) of the tested compounds were determined by the agar dilution method in Middlebrook 7H11 agar (Difco, Becton Dickinson, Sparks, MD, USA) supplemented with oleic acid, albumin, dextrose and catalase (OADC, Difco), as previously reported with slight modifications.[22] *M. tuberculosis* H37Ra ATCC 25177 was maintained in slants of Lowenstein-Jensen medium (Difco), subcultured in Middlebrook 7H9 broth (Difco) supplemented with 10% albumin, dextrose and catalase (ADC, Difco) and 0.04% Tween-80. Cultures were incubated at 37 °C and 5% CO₂ for 2 weeks. The bacteria were harvested by centrifugation (2000 x g, 10 min), resuspended in Middlebrook 7H9 broth with 0.04% Tween-80 and sonicated in a bath-type sonicator to disrupt the clumps. The inoculum was adjusted to 3x10⁶ CFU/mL by comparison with a McFarland No. 1 turbidity standard, and an aliquot of 100 µL of the bacterial suspension containing 3x10⁵ CFU was seeded on to 7H11 agar with OADC 10% in 24-well plates containing the testing compounds at concentrations ranging between 64 and 0.016 µg/mL. The inoculum size was also confirmed by seeding 100 µL of the bacteria suspension in Middlebrook 7H11 agar plates and incubated for 21 days at 37 °C in 5% CO₂. Isoniazid served as reference drug. Plates were incubated at 37

°C in 5% CO₂ for 28 days. MICs were defined as the lowest concentration at which no growth was observed.

5. ACKNOWLEDGEMENTS

The authors wish also to thank the OpenEye Free Academic Licensing Program for providing a free academic license for molecular modeling and chemoinformatics software.

6. REFERENCES

- [1] Global Tuberculosis Report 2015. WHO. ISBN 978 92 4 156505 9, in, World Health Organization.
- [2] G. Sotgiu, A. Matteelli, H. Getahun, E. Girardi, M. Sane Schepisi, R. Centis, G.B. Migliori, Monitoring toxicity in individuals receiving treatment for latent tuberculosis infection: a systematic review versus expert opinion, *Eur. Respir. J.*, 45 (2015) 1170-1173.
- [3] G. Piccaro, P. Filippini, F. Giannoni, L. Scipione, S. Tortorella, D. De Vita, P. Mellini, L. Fattorini, Activity of drugs against dormant *Mycobacterium tuberculosis*, *J. Chemother.*, 23 (2011) 175-178.
- [4] Centers for Disease Control and Prevention. The Difference Between Latent TB Infection and TB Disease. <http://www.cdc.gov/tb/publications/factsheets/general/lbtbandactivetb.htm> (accessed October 17, 2015).
- [5] Centers for Disease Control and Prevention. <http://www.cdc.gov/tb/topic/treatment/> (accessed October 17, 2015).
- [6] P.R. Baldwin, A.Z. Reeves, K.R. Powell, R.J. Napier, A.I. Swimm, A. Sun, K. Giesler, B. Bommarius, T.M. Shinnick, J.P. Snyder, D.C. Liotta, D. Kalman, Monocarbonyl analogs of curcumin inhibit growth of antibiotic sensitive and resistant strains of *Mycobacterium tuberculosis*, *Eur. J. Med. Chem.*, 92 (2015) 693-699.
- [7] R. Mahajan, Bedaquiline: First FDA-approved tuberculosis drug in 40 years, *Int J Appl Basic Med Res*, 3 (2013) 1-2.
- [8] A. Anand, R.J. Naik, H.M. Revankar, M.V. Kulkarni, S.R. Dixit, S.D. Joshi, A click chemistry approach for the synthesis of mono and bis aryloxy linked coumarinyl triazoles as anti-tubercular agents, *Eur. J. Med. Chem.*, 105 (2015) 194-207.

- [9] D.S. Reddy, K.M. Hosamani, H.C. Devarajegowda, Design, synthesis of benzocoumarin-pyrimidine hybrids as novel class of antitubercular agents, their DNA cleavage and X-ray studies, *Eur. J. Med. Chem.*, 101 (2015) 705-715.
- [10] R.R. Yadav, S.I. Khan, S. Singh, I.A. Khan, R.A. Vishwakarma, S.B. Bharate, Synthesis, antimalarial and antitubercular activities of meridianin derivatives, *Eur. J. Med. Chem.*, 98 (2015) 160-169.
- [11] A. Penta, S. Franzblau, B.J. Wan, S. Murugesan, Design, synthesis and evaluation of diarylpiperazine derivatives as potent anti-tubercular agents, *Eur. J. Med. Chem.*, 105 (2015) 238-244.
- [12] F. Manetti, M. Magnani, D. Castagnolo, L. Passalacqua, M. Botta, F. Corelli, M. Saddi, D. Deidda, A. De Logu, Ligand-based virtual screening, parallel solution-phase and microwave-assisted synthesis as tools to identify and synthesize new inhibitors of mycobacterium tuberculosis, *ChemMedChem*, 1 (2006) 973-989.
- [13] D. Castagnolo, A. De Logu, M. Radi, B. Bechi, F. Manetti, M. Magnani, S. Supino, R. Meleddu, L. Chisu, M. Botta, Synthesis, biological evaluation and SAR study of novel pyrazole analogues as inhibitors of Mycobacterium tuberculosis, *Bioorg. Med. Chem.*, 16 (2008) 8587-8591.
- [14] D. Castagnolo, F. Manetti, M. Radi, B. Bechi, M. Pagano, A. De Logu, R. Meleddu, M. Saddi, M. Botta, Synthesis, biological evaluation, and SAR study of novel pyrazole analogues as inhibitors of Mycobacterium tuberculosis: part 2. Synthesis of rigid pyrazolones, *Bioorg. Med. Chem.*, 17 (2009) 5716-5721.
- [15] D. Castagnolo, M. Radi, F. Dessi, F. Manetti, M. Saddi, R. Meleddu, A. De Logu, M. Botta, Synthesis and biological evaluation of new enantiomerically pure azole derivatives

as inhibitors of *Mycobacterium tuberculosis*, *Bioorg. Med. Chem. Lett.*, 19 (2009) 2203-2205.

[16] M. Biava, G.C. Porretta, G. Poce, A. De Logu, R. Meleddu, E. De Rossi, F. Manetti, M. Botta, 1,5-Diaryl-2-ethyl pyrrole derivatives as antimycobacterial agents: design, synthesis, and microbiological evaluation, *Eur. J. Med. Chem.*, 44 (2009) 4734-4738.

[17] M. Biava, G.C. Porretta, G. Poce, C. Battilocchio, S. Alfonso, A. De Logu, N. Serra, F. Manetti, M. Botta, Identification of a novel pyrrole derivative endowed with antimycobacterial activity and protection index comparable to that of the current antitubercular drugs streptomycin and rifampin, *Bioorg. Med. Chem.*, 18 (2010) 8076-8084.

[18] S.A. Hudson, K.J. McLean, A.W. Munro, C. Abell, *Mycobacterium tuberculosis* cytochrome P450 enzymes: a cohort of novel TB drug targets, *Biochem. Soc. Trans.*, 40 (2012) 573-579.

[19] Accelrys, Inc. 2000 Catalyst 4.6 Program (Accelrys, Inc. San Diego, CA).

[20] F.H. Allen, C.M. Bird, R.S. Rowland, P.R. Raithby, Hydrogen-bond acceptor and donor properties of divalent sulfur (Y-S-Z and R-S-H), *Acta Crystallographica Section B-Structural Science*, 53 (1997) 696-701.

[21] T.G. Heafield, G. Hopkins, L. Hunter, Hydrogen Bonds involving the Sulphur Atom, *Nature*, 149 (1942).

[22] A. De Logu, M. Saddi, V. Onnis, C. Sanna, C. Congiu, R. Borgna, M.T. Cocco, In vitro antimycobacterial activity of newly synthesised S-alkylisothiosemicarbazone derivatives and synergistic interactions in combination with rifamycins against *Mycobacterium avium*, *Int. J. Antimicrob. Agents*, 26 (2005) 28-32.

- [23] D. De Vita, L. Scipione, S. Tortorella, P. Mellini, B. Di Rienzo, G. Simonetti, F.D. D'Auria, S. Panella, R. Cirilli, R. Di Santo, A.T. Palamara, Synthesis and antifungal activity of a new series of 2-(1H-imidazol-1-yl)-1-phenylethanol derivatives, *Eur. J. Med. Chem.*, 49 (2012) 334-342.
- [24] L. Friggeri, T.Y. Hargrove, G. Rachakonda, A.D. Williams, Z. Wawrzak, R. Di Santo, D. De Vita, M.R. Waterman, S. Tortorella, F. Villalta, G.I. Lepesheva, Structural Basis for Rational Design of Inhibitors Targeting *Trypanosoma cruzi* Sterol 14 α -Demethylase: Two Regions of the Enzyme Molecule Potentiate Its Inhibition, *J. Med. Chem.*, 57 (2014) 6704-6717.
- [25] L. Friggeri, L. Scipione, R. Costi, M. Kaiser, F. Moraca, C. Zamperini, B. Botta, R. Di Santo, D. De Vita, R. Brun, S. Tortorella, New Promising Compounds with in Vitro Nanomolar Activity against *Trypanosoma cruzi*, *Acs Medicinal Chemistry Letters*, 4 (2013) 538-541.
- [26] I.C. Lennon, J.A. Ramsden, An efficient catalytic asymmetric route to 1-aryl-2-imidazol-1-yl-ethanols, *Org. Process Res. Dev.*, 9 (2005) 110-112.
- [27] N. Clauson-Kaas, Z. Tyle, Preparation of Cis- and Trans 2,5-Dimethoxy-2-(acetamidomethyl)-2,5-dihydrofuran, of Cis- and Trans 2,5-Dimethoxy-2-(acetamidomethyl)-tetrahydrofuran and of 1-Phenyl-2-(acetamidomethyl)-pyrrole., *Acta Chem. Scand.*, 6 (1952) 667-670.
- [28] G. Cruciani, E. Carosati, B. De Boeck, K. Ethirajulu, C. Mackie, T. Howe, R. Vianello, MetaSite: understanding metabolism in human cytochromes from the perspective of the chemist, *J. Med. Chem.*, 48 (2005) 6970-6979.

- [29] G. Cruciani, M. Baroni, P. Benedetti, L. Goracci, C.G. Fortuna, Exposition and reactivity optimization to predict sites of metabolism in chemicals, *Drug Discov Today Technol*, 10 (2013) e155-165.
- [30] G. Cruciani, A. Valeri, L. Goracci, R.M. Pellegrino, F. Buonerba, M. Baroni, Flavin monooxygenase metabolism: why medicinal chemists should matter, *J. Med. Chem.*, 57 (2014) 6183-6196.
- [31] OpenEye, ROCS 3.2.0.4 OpenEye Scientific Software, Santa Fe, NM. <http://www.eyesopen.com>
- [32] P.C. Hawkins, A.G. Skillman, A. Nicholls, Comparison of shape-matching and docking as virtual screening tools, *J. Med. Chem.*, 50 (2007) 74-82.
- [33] J. Mao, H. Eoh, R. He, Y. Wang, B. Wan, S.G. Franzblau, D.C. Crick, A.P. Kozikowski, Structure-activity relationships of compounds targeting mycobacterium tuberculosis 1-deoxy-D-xylulose 5-phosphate synthase, *Bioorg. Med. Chem. Lett.*, 18 (2008) 5320-5323.
- [34] S. Ananthan, E.R. Faaleolea, R.C. Goldman, J.V. Hobrath, C.D. Kwong, B.E. Laughon, J.A. Maddry, A. Mehta, L. Rasmussen, R.C. Reynolds, J.A. Secrist, 3rd, N. Shindo, D.N. Showe, M.I. Sosa, W.J. Suling, E.L. White, High-throughput screening for inhibitors of Mycobacterium tuberculosis H37Rv, *Tuberculosis (Edinb.)*, 89 (2009) 334-353.
- [35] W.J. Egan, K.M. Merz, Jr., J.J. Baldwin, Prediction of drug absorption using multivariate statistics, *J. Med. Chem.*, 43 (2000) 3867-3877.
- [36] OpenEye, OMEGA 2.5.1.4: OpenEye Scientific Software, Santa Fe, NM. <http://www.eyesopen.com>

[37] P.C. Hawkins, A.G. Skillman, G.L. Warren, B.A. Ellingson, M.T. Stahl, Conformer generation with OMEGA: algorithm and validation using high quality structures from the Protein Databank and Cambridge Structural Database, *J. Chem. Inf. Model.*, 50 (2010) 572-584.

[38] Accelrys, Inc. 2000 DiscoveryStudio 2.5 (Accelrys, Inc. San Diego, CA).

[39] J.J. Irwin, T. Sterling, M.M. Mysinger, E.S. Bolstad, R.G. Coleman, ZINC: a free tool to discover chemistry for biology, *J. Chem. Inf. Model.*, 52 (2012) 1757-1768.

[40] D.F. Veber, S.R. Johnson, H.Y. Cheng, B.R. Smith, K.W. Ward, K.D. Kopple, Molecular properties that influence the oral bioavailability of drug candidates, *J. Med. Chem.*, 45 (2002) 2615-2623.

7. Figure Legends

Figure 1. Common feature pharmacophore model used as query in virtual screening. The model is composed of five features: RA = Ring Aromatic in orange meshes; HydArom = Hydrophobic Aromatic in cyan meshes; HydAli = Hydrophobic aliphatic in blue meshes and HBA = H-Bond Acceptor in green meshes. Grey meshes indicated the exclusion volumes. In the left-hand panel, the alignment between the common feature pharmacophore and one of the most potent compounds included in the training set (MIC < 0.125 µg/mL) is shown.

Figure 2: A, query molecules: **24** = Hit compound identified in this work, **a** = compound from Ananthan et al., **b** and **c** = molecules from Mao et al.; B, query generated from the four molecules; C, structure of compound **42** with activity of 2 µg/mL

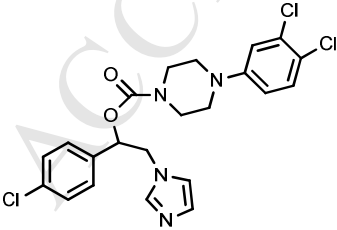
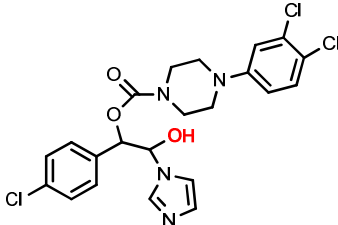
Figure 3: The 3-phenylpyrazolo[1-5a]pyrimidin-7(4H)-one scaffold used for the structure activity relationship

Table 1. *In vitro* antitubercular activity of tested compounds. Minimum Inhibitory Concentration (MIC) values against *M. tuberculosis* H37Ra ATCC 25177 were determined by the agar dilution method and are given in $\mu\text{g/mL}$.

Cmpd	MIC	Cmpd	MIC
1	64	14	32
(S)- 2	32	15	32
(S)- 3	16	16	64
(S)- 4	16	17	32
(S)- 5a	64	18	32
(S)- 5b	64	19	32
(S)- 5c	32	20	32
5d	16	21	32
(S)- 5e	16	22	32
(S)- 5f	16	23	32
(S)- 5g	16	24	8
(S)- 5h	16	25	64
5i	4	26	32
(S)- 5l	8	27	32
(S)- 5m	16	28	64

(S)-5n	16	29	32
(S)-6	16	30	>64
(S)-7	16	31	32
8	64	32	32
9	64	33	32
10	32	34	64
11	32	35	64
12	32	36	64
13	32		

Table 2: *In vitro* metabolic stability of 5i

	Metabolic stability ^[a]	Major metabolites ^[b]
 <p>5i</p>	99.0 %	M1=M+16 (1.0 %)
		

[a] Expressed as percentage of unmodified parent drug. [b] M = mass of the parent drug; M1 = experimental mass of the identified metabolites.

Table 3: *In vitro* antitubercular activity of **37-49**. Minimum inhibitory concentration (MIC) values against *M. tuberculosis* H37Ra ATCC 25177 were determined by the agar dilution method and are given in $\mu\text{g/mL}$.

<i>compd</i>	MIC	<i>compd</i>	MIC
37	8	44	64
38	32	45	32
39	32	46	32
40	16	47	64
41	32	48	16
42	2	49	8
43	32		

Table 4: Modification of the filter

<i>Modification</i>	<i>Default</i>	<i>Value after modification</i>
<i>MW min</i>	200	170
<i>MAX LogP</i>	6.0	6.75
<i>Min solub</i>	moderately	poorly
<i>MAX Alkyl halide</i>	0	3
<i>MAX Nitro</i>	0	1
<i>MAX Halide</i>	6	9
<i>MAX Thiourea</i>	0	1
<i>Predict aggregator</i>	True	False
<i>GSK VEBER^[28]</i>	True	False
<i>PHARMACOPIA^[26]</i>	True	False

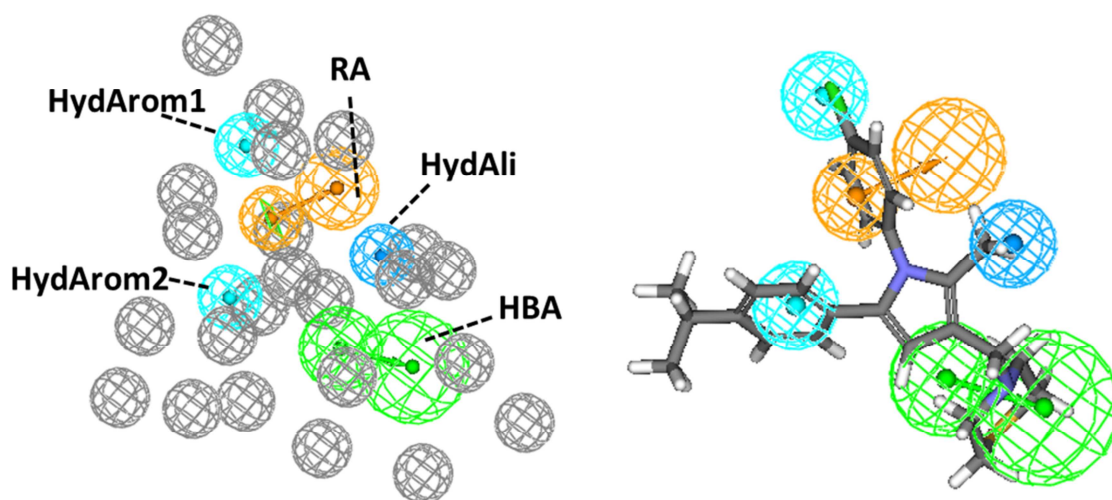


Figure 1. Common feature pharmacophore model used as query in virtual screening. The model is composed of five features: RA = Ring Aromatic in orange meshes; HydArom = Hydrophobic Aromatic in cyan meshes; HydAli = Hydrophobic aliphatic in blue meshes and HBA = H-Bond Acceptor in green meshes. Grey meshes indicated the exclusion volumes. In the left-hand panel, the alignment between the common feature pharmacophore and one of the most potent compounds included in the training set (MIC < 0.125 $\mu\text{g}/\text{mL}$) is shown.

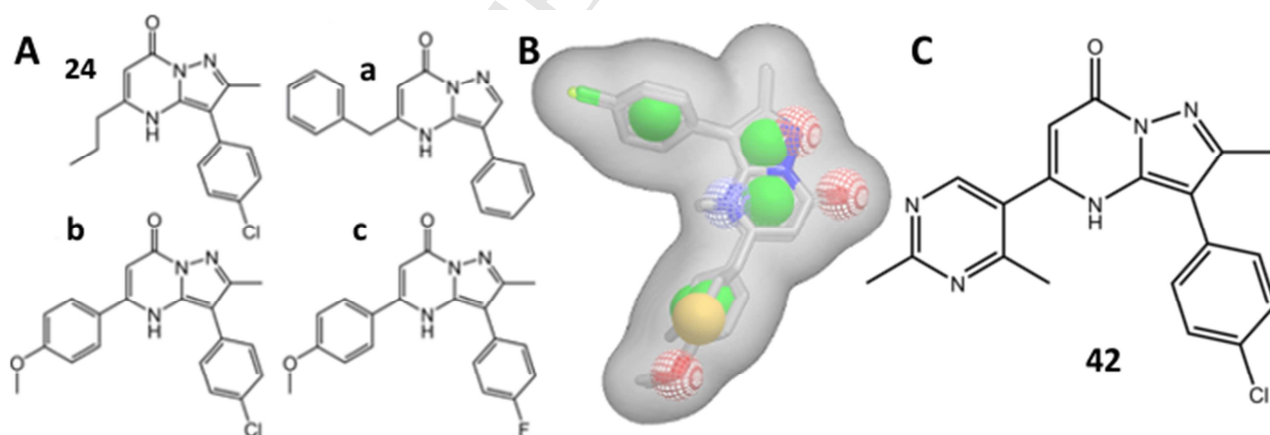


Figure 2: A, query molecules: **24** = Hit compound identified in this work, **a** = compound from Ananthan et al., **b** and **c** = molecules from Mao et al.; B, query generated from the four molecules; C, structure of compound **42** with activity of 2 $\mu\text{g}/\text{mL}$

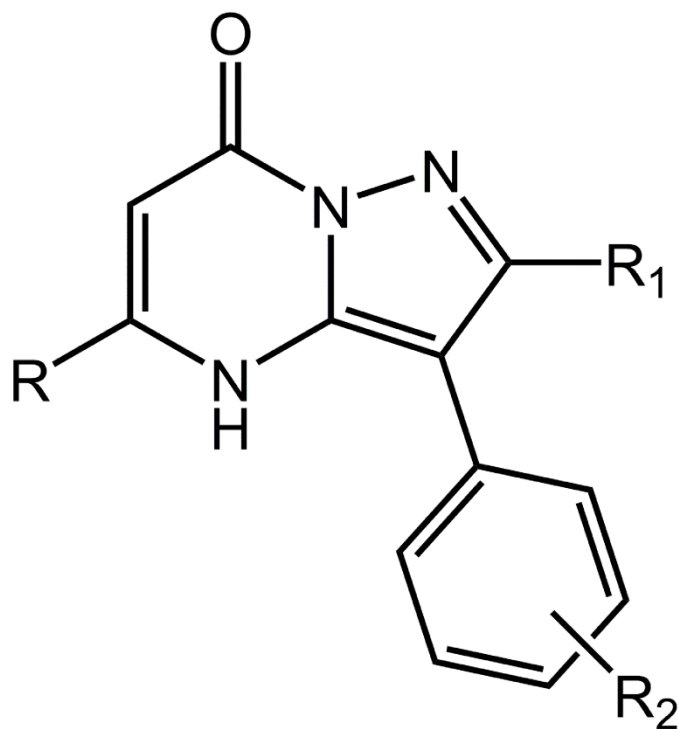
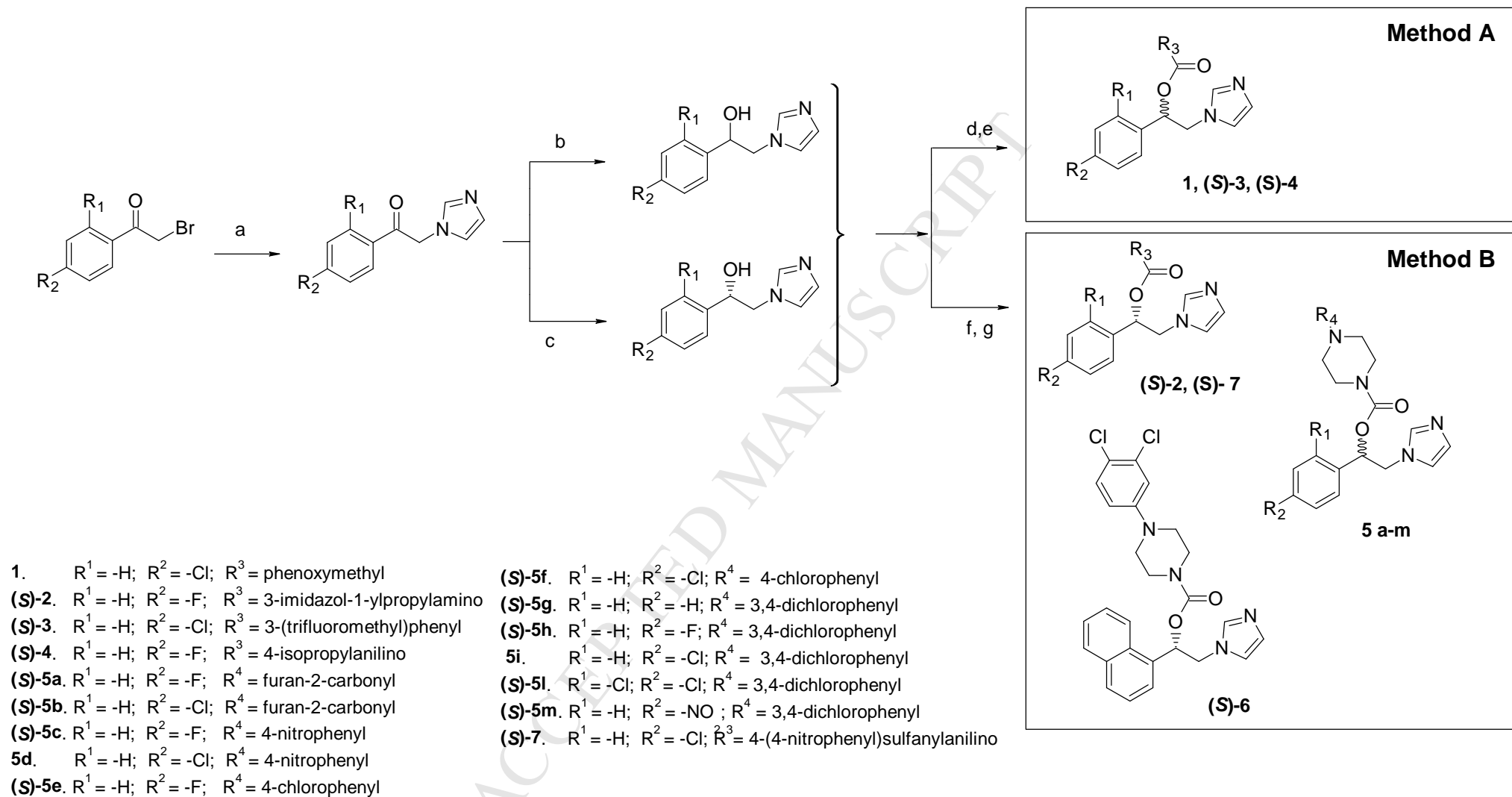
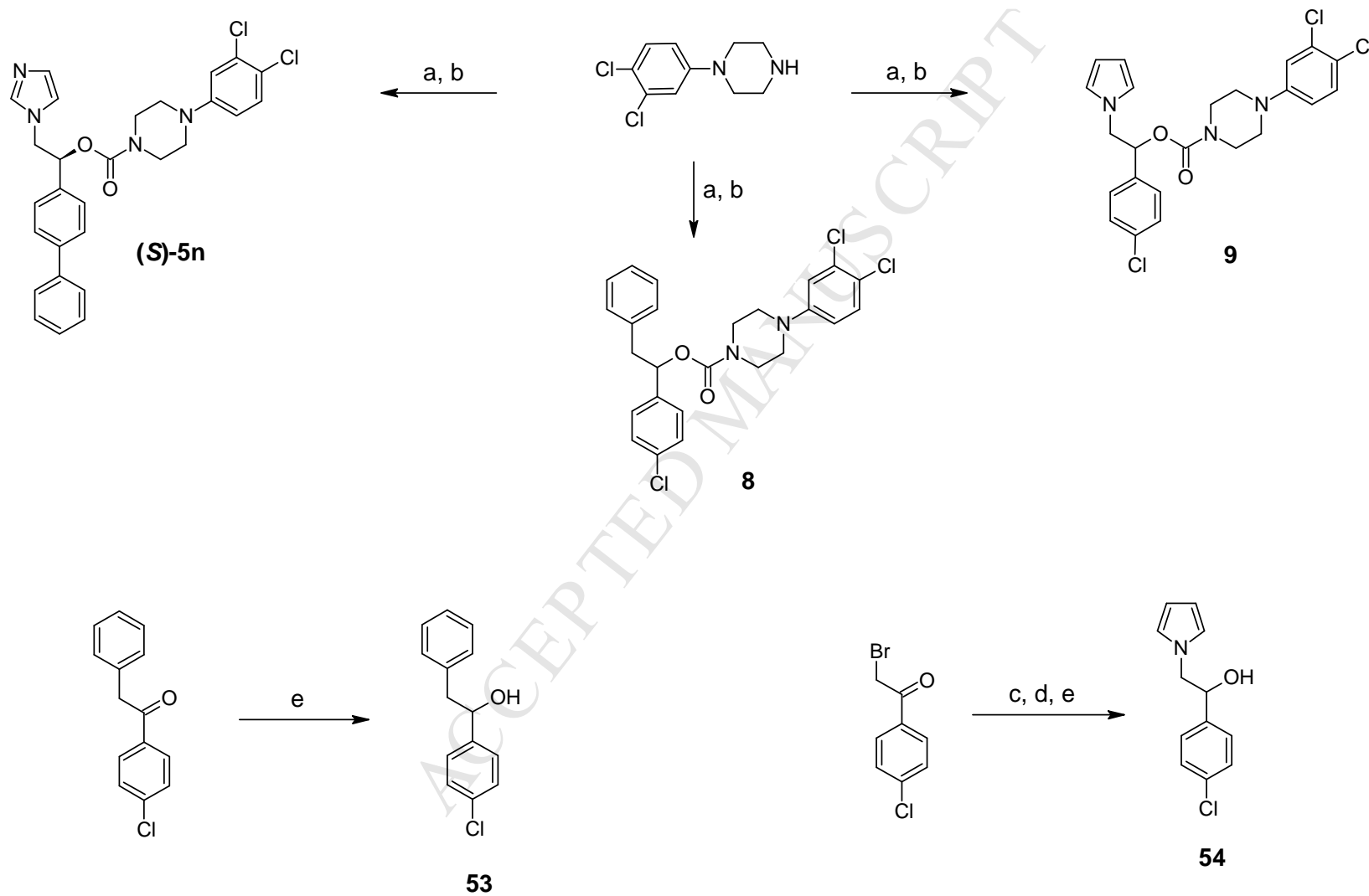


Figure 3: The 3-phenylpyrazolo[1-5a]pyrimidin-7(4H)-one scaffold used for the structure activity relationship



Scheme 1. Synthesis of compounds **1-4**, **5a-m**, **6** and **7** (as racemates or enantiomers). *Reagents and conditions:* a) imidazole, DMF, 2h, 0°C; b) NaBH₄, MeOH, 2h, reflux; c) RuCl(p-cymene)[(R,R)-Ts-DPEN], HCOOH, TEA, N_{2(g)}, CH₂Cl₂, 26 h, 40°C; d) NaH, anhydrous CH₃CN, 2 h, RT; e) phenoxyacetyl chloride (**1**), 3-

(trifluoromethyl)benzoyl chloride ((**S**-3) or 4-isopropylphenyl isocyanate ((**S**-4), 24-48 h, RT; f) triphosgene, anhydrous CH₃CN, overnight, RT; g) opportune amine, TEA, anhydrous CH₃CN, overnight, RT.



Scheme 2. Synthesis of **(S)-5n, 8** and **9**. *Reagents and conditions:* a) triphosgene, pyridine, CH₂Cl₂ 3 h, RT; b) opportune alcohol (**51**, **53** or **54**) TEA, CH₂Cl₂, overnight, RT; c) hexamethylenetetramine, CH₂Cl₂ 2 h, RT, then HCl 6M, EtOH, 3 days, RT; d) 2,5-dimethoxytetrahydrofuran, DMF, 5 min, 150-160°C; e) Na BH₄, MeOH / CH₂Cl₂ (1:1), 1 h, RT.

ACCEPTED MANUSCRIPT